

# Angular momentum evolution of young low-mass stars and brown dwarfs: observations and theory

**Jérôme Bouvier**

Observatoire de Grenoble

**Sean P. Matt**

Exeter University

**Subhanjoy Mohanty**

Imperial College London

**Aleks Scholz**

University of St Andrews

**Keivan G. Stassun**

Vanderbilt University

**Claudio Zanni**

Osservatorio Astrofisico di Torino

This chapter aims at providing the most complete review of both the emerging concepts and the latest observational results regarding the angular momentum evolution of young low-mass stars and brown dwarfs. In the time since *Protostars & Planets V*, there have been major developments in the availability of rotation period measurements at multiple ages and in different star-forming environments that are essential for testing theory. In parallel, substantial theoretical developments have been carried out in the last few years, including the physics of the star-disk interaction, numerical simulations of stellar winds, and the investigation of angular momentum transport processes in stellar interiors. This chapter reviews both the recent observational and theoretical advances that prompted the development of renewed angular momentum evolution models for cool stars and brown dwarfs. While the main observational trends of the rotational history of low mass objects seem to be accounted for by these new models, a number of critical open issues remain that are outlined in this review.

## 1. INTRODUCTION

The angular momentum content of a newly born star is one of the fundamental quantities, like mass and metallicity, that durably impacts on the star's properties and evolution. Rotation influences the star's internal structure, energy transport, and the mixing processes in the stellar interior that are reflected in surface elemental abundances. It is also the main driver for magnetic activity, from X-ray luminosity to UV flux and surface spots, that is the ultimate source of stellar winds. Studying the initial angular momentum content of stars and its evolution throughout the star's lifetime brings unique clues to the star formation process, to the accretion/ejection phenomenon in young stellar objects, to the history and future of stellar activity and its impact on surrounding planets, and to physical processes that redistribute angular momentum in stellar interiors.

Spectacular progress has been made, both on the obser-

vational and theoretical sides, on the issue of the angular momentum evolution of young stellar objects since *Protostars & Planets V*. On the observational side, thousands of new rotational periods have been derived for stars over the entire mass range from solar-type stars down to brown dwarfs at nearly all stages of evolution between birth and maturity. The picture we have of the rotational evolution of low-mass and very low-mass stars and brown dwarfs has never been as well documented as of today. On the theoretical side, recent years have seen a renaissance in numerical simulations of magnetized winds that are the prime agent of angular momentum loss, new attempts have been made to understand how young stars exchange angular momentum with their disks via magnetic interactions, and new insights have been gained on the way angular momentum is transported in stellar interiors.

In the following sections, we review the latest developments which shed new light on the processes governing

TABLE 1  
POST-PPV ROTATIONAL PERIOD DISTRIBUTIONS FOR YOUNG ( $\leq 1$  GYR) STARS

Reference	Target	Age (Myr)	Mass range ( $M_{\odot}$ )	$N_{\star}$
<i>Grankin (2013)</i>	Taurus	1-3	0.4-1.6	61
<i>Xiao et al. (2012)</i>	Taurus	1-3	0.3-1.2	18
<i>Artemenko et al. (2012)</i>	Various SFRs	1-5	0.3-3.0	52
<i>Henderson and Stassun (2012)</i>	NGC 6530	2	0.2-2.0	244
<i>Rodríguez-Ledesma et al. (2009)</i>	ONC	2	0.015-0.5	487
<i>Affer et al. (2013)</i>	NGC 2264	3	0.2-3.0	209
<i>Cody and Hillenbrand (2010)</i>	$\sigma$ Ori	3	0.02-1.0	64
<i>Littlefair et al. (2010)</i>	Cep OB3b	4-5	0.1-1.3	475
<i>Irwin et al. (2008a)</i>	NGC 2362	5	0.1-1.2	271
<i>Messina et al. (2011)</i>	Young assoc.	6-40	0.2-1.0	80
<i>Messina et al. (2010)</i>	Young assoc.	8-110	0.2-1.0	165
<i>Moraux et al. (2013)</i>	h Per	13	0.4-1.4	586
<i>Irwin et al. (2008b)</i>	NGC 2547	40	0.1-0.9	176
<i>Scholz et al. (2009)</i>	IC 4665	40	0.05-0.5	20
<i>Hartman et al. (2010)</i>	Pleiades	125	0.4-1.3	383
<i>Irwin et al. (2009)</i>	M 50	130	0.2-1.1	812
<i>Irwin et al. (2007)</i>	NGC 2516	150	0.15-0.7	362
<i>Meibom et al. (2009)</i>	M35	150	0.6-1.6	310
<i>Sukhbold and Howell (2009)</i>	NGC 2301	210	0.5-1.0	133
<i>Meibom et al. (2011b)</i>	M34	220	0.6-1.2	83
<i>Hartman et al. (2009)</i>	M 37	550	0.2-1.3	371
<i>Scholz and Eislöffel (2007)</i>	Praesepe	578	0.1-0.5	5
<i>Agüeros et al. (2011)</i>	Praesepe	578	0.27-0.74	40
<i>Scholz et al. (2011)</i>	Praesepe	578	0.16-0.42	26
<i>Collier Cameron et al. (2009)</i>	Coma Ber	591	FGK	46
<i>Delorme et al. (2011)</i>	Praesepe/Hyades	578/625	FGK	52/70
<i>Meibom et al. (2011a)</i>	NGC 6811	1000	FGK	71
<i>Irwin et al. (2011)</i>	Field M dwarfs	500-13000	0.1-0.3	41
<i>Kiraga and Stepien (2007)</i>	Field M dwarfs	3000-10000	0.1-0.7	31

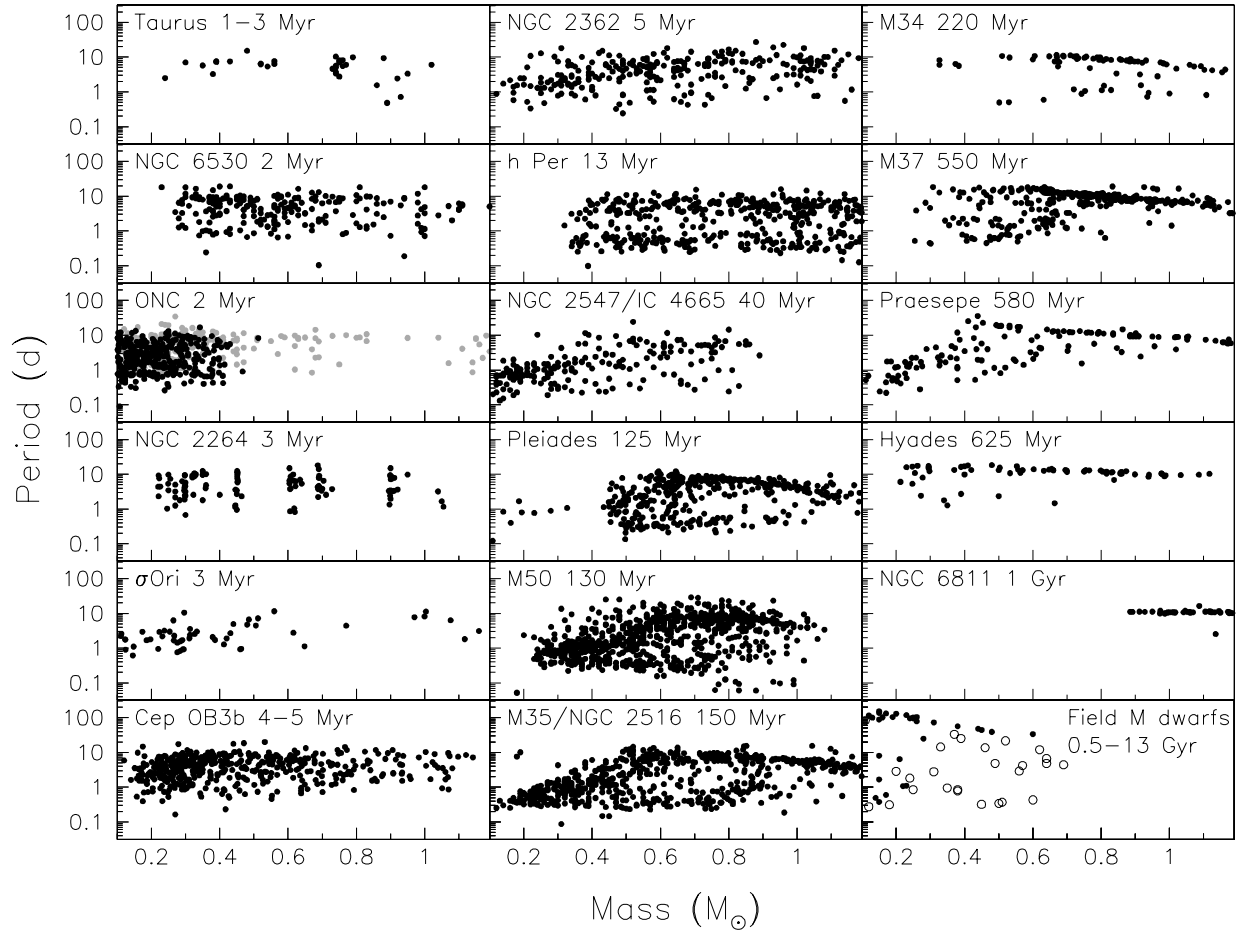


Fig. 1.— The rotational period distribution of low mass stars derived since Protostars & Planets V in star forming regions, young open clusters, and in the field. The panels are ordered by increasing age, from top to bottom and left to right. The ONC panel includes previous measurements by *Herbst et al. (2002)* shown as grey dots. In the lower right panel, young disk M dwarfs are shown as open circles, old disk ones as filled circles. References are listed in Table 1.

the angular momentum evolution of young stars and brown dwarfs, and also provide important context for other Protostars & Planets VI chapters to explore possible connections between the rotational history of stars and the formation, migration and evolution of planetary systems (star-disk interaction, inner disk warps and cavities, planet engulfment, irradiation of young planets, etc.). In Section 2, we review the latest advances in the derivation of rotation rates for low mass stars and brown dwarfs from birth to the early main sequence. In Section 3, we provide an account of the physical mechanisms thought to dictate the evolution of stellar rotation during the pre-main sequence (PMS) and early main sequence (MS), including star-disk interaction, stellar winds, and angular momentum transport in stellar interiors. In Section 4, we discuss various classes of angular momentum evolution models that implement the latest theoretical developments to account for the observed evolution of stellar rotation in cool stars and brown dwarfs.

## 2. OBSERVATIONAL STUDIES OF STELLAR ROTATION

The measurement of rotational periods for thousands of stars in molecular clouds and young open clusters provide the best way to trace their angular momentum evolution from about 1 Myr to 1 Gyr. This section discusses the observational studies of stellar rotation performed since *Herbst et al.*'s (2007) PPV review, for solar-type stars and lower mass stars, down to the brown dwarf regime.

### 2.1 Solar-mass and low-mass stars

In the last 7 years, more than 5,000 new rotational periods have been measured for cool stars in star forming regions and young open clusters, over an age range from 1 Myr to 1 Gyr. In parallel, dedicated photometric monitoring of nearby M dwarfs, aimed at planetary transit searches, have reported tens of periods for the field very low-mass population over the age range 1-13 Gyr. These recent studies are listed in Table 1 while Figure 1 provides a graphical summary of the results. A compilation of prior results was published by *Irwin and Bouvier* (2009).

In addition, Kepler's and CoRoT's long term monitoring has provided rotation periods for more than 10,000 GKM field dwarfs (e.g., *Nielsen et al.* 2013; *McQuillan et al.* 2013; *Harrison et al.* 2012; *Affer et al.* 2012). These results offer a global view of stellar rotation as a function of mass on the main sequence, exhibiting a large dispersion at each spectral type, which possibly reflects the age distribution of the stellar samples.

The evolution of rotational distributions from 1 Myr to the old disk population shown in Fig. 1 reveals a number of features:

- The initial distribution of spin rates at an age of about 2 Myr is quite wide over the whole mass range from 0.2 to 1.0  $M_{\odot}$ , with the bulk of rotational periods

ranging from 1 to 10 days. The lower envelope of the period distribution is located at about 0.7 days, which corresponds to about 40-50% of the break-up limit over the mass range 0.2-1.0  $M_{\odot}$ . The origin of the initial scatter of stellar angular momentum for low mass stars remains an open issue and probably reflects physical processes taking place during the embedded protostellar stage. *Gallet and Bouvier* (2013) suggested that the dispersion of initial angular momenta may be linked to the protostellar disk mass.

- From 1 to 5 Myr, i.e., during the early PMS evolution, the rotation rates of solar-type stars hardly evolve. In contrast, the lowest mass stars significantly spin up. *Henderson and Stassun* (2012) suggested that the increasing period-mass slope for lower mass stars can be used as an age proxy for very young clusters. *Littlefair et al.* (2010), however, reported that the similarly aged (5 Myr) NGC 2362 and Cep OB3b clusters exhibit quite a different rotational period distribution at low masses, which may point to the impact of environmental effects on rotation properties.
- Past the end of the PMS accretion phase, the rotational distribution of the 13 Myr h Per cluster members is remarkably flat over the 0.4-1.2  $M_{\odot}$  range. The lower envelope of the period distribution, now located at about 0.2-0.3d, bears strong evidence for PMS spin up, as the freely evolving stars contract towards the ZAMS. In contrast, the slow rotators still retain periods close to 8-10 days, a result interpreted as evidence for core-envelope decoupling in these stars (*Morax et al.* 2013). Similar results are seen in the 40 Myr clusters IC 4665 and NGC 2547, with the addition of very low mass stars that are faster rotators and exhibit a steep period-mass relationship.
- Once on the early MS (0.1-0.6 Gyr), a well-defined sequence of slow rotators starts to appear over the mass range 0.6-1.1  $M_{\odot}$  while the lower mass stars still retain fast rotation. This suggests a spin down timescale of order of a few 0.1 Gyr for solar-type stars, as angular momentum is carried away by magnetized winds. The development of a slow rotator sequence and its gradual evolution towards longer periods indeed serves as a basis to main sequence gyrochronology (*Barnes* 2007).
- By an age of 0.5-0.6 Gyr, all solar-type stars down to a mass of 0.6  $M_{\odot}$  have spun down, thus yielding a tight period-mass relationship, with the rotation rate decreasing towards lower masses (*Delorme et al.* 2011). In contrast, the very low mass stars still exhibit a large scatter in spin rates at that age (*Agüeros et al.* 2011). It is only in the old disk population, by about 10 Gyr, that the majority of lowest mass stars join the slow rotator sequence (*Irwin et al.* 2011). Clearly, the spin down timescale is a strong function of stellar mass, being much longer for the lowest

mass stars than for solar-type ones (e.g., *McQuillan et al.* 2013).

A long-standing and somewhat controversial issue remains the so-called “disk-locking” process, i.e., the observational evidence that stars magnetically interacting with their accretion disk during the first few Myr of PMS evolution are prevented from spinning up in spite of contracting towards the ZAMS (e.g., *Rebull et al.* 2004). A number of post-PPV studies tend to support the view that, at a given age, disk-bearing PMS stars are, on average, slower rotators than diskless ones, with periods typically in the range from 3 to 10 days for the former, and between 1 and 7 days for the latter (e.g., *Affer et al.* 2013; *Xiao et al.* 2012; *Henderson and Stassun* 2012; *Littlefair et al.* 2010; *Rodríguez-Ledesma et al.* 2009; *Irwin et al.* 2008a; *Cieza and Baliber* 2007). However, in all star forming regions investigated so far, there is a significant overlap between the rotational distributions of classical and weak-line T Tauri stars. Furthermore, *Cody and Hillenbrand* (2010) failed to find any evidence for a disk-rotation connection among the very low mass members of the 3 Myr  $\sigma$  Ori cluster, which suggests it may only be valid over a restricted mass range.

The lack of a clear relationship between rotation and disk accretion may have various causes. Observationally, the determination of rotational period distributions relies on the assumption that the photometric periods derived from monitoring studies arise from surface spot modulation and therefore accurately reflect the star’s rotational period. Recently, *Artemenko et al.* (2012) questioned the validity of this assumption for classical T Tauri stars. Based on the comparison of photometric periods and  $v \sin i$  measurements, they claimed that in a fraction of classical T Tauri stars the measured periods correspond to the Keplerian motion of obscuring circumstellar dust in the disk and are significantly longer than the stellar rotational periods (see also *Percy et al.* 2010). *Alencar et al.* (2010), however, found that the photometric periods of classical T Tauri stars undergoing cyclical disk obscuration were statistically similar to those of classical T Tauri stars dominated by surface spots, thus suggesting that the obscuring dust is located close to the co-rotation radius in the disk.

On the theoretical side, the star-disk interaction may impact the star’s rotation rate in various ways, depending in particular on the ratio between the disk truncation and co-rotation radii. *Le Blanc et al.* (2011) have modeled the spectral energy distribution of young stars in IC 348 in an attempt to derive the disk inner radius and evaluate its relationship with the star’s rotational period. No clear trend emerges from the ratio of inner disc radius to corotation radius when comparing slow and fast rotators. It should be cautioned, however, that SED modeling actually measures the inner *dusty* disk radius, while the *gaseous* disc may extend further in (e.g., *Carr* 2007). Also, scattered light in the near-IR may substantially alter the measurement of inner dust disk radius in T Tauri stars (*Pinte et al.* 2008).

## 2.2 Very low-mass stars and brown dwarfs

Significant progress has recently been made in evaluating the rotational properties of very low mass objects (VLM, masses below  $\sim 0.3 M_{\odot}$ ), including brown dwarfs (BDs), i.e., objects with masses too low to sustain stable hydrogen burning ( $M < 0.08 M_{\odot}$ ). In the last Protostars and Planets review on this subject (*Herbst et al.* 2007), about 200 periods for VLM objects in the ONC and NGC2264, two 1-3 Myr old star forming regions, were discussed. In addition, smaller samples in other clusters were already available at that time. For brown dwarfs the total sample was limited to about 30 periods, only a handful for ages  $> 10$  Myr, complemented by  $v \sin i$  measurements. We summarize in this Section the most recent advances regarding the measurement of spin rates for very low mass stars and brown dwarfs, and recapitulate the emerging picture for the angular momentum evolution in the VLM domain.

**Star forming regions:** For the Orion Nebula Cluster, at an age of 1-2 Myr, *Rodríguez-Ledesma et al.* (2009) have published several hundred new VLM periods. This includes more than 100 periods for brown dwarf candidates, the largest BD period sample in any region studied so far. A new period sample across the stellar/substellar regime in the slightly older  $\sigma$  Ori cluster has been presented by *Cody and Hillenbrand* (2010), including about 40 periods for VLM objects. In addition, the period sample from the *Monitor* project in the 4-5 Myr old cluster NGC2362 contains about 20-30 periods in the VLM regime (*Irwin et al.* 2008a) and the new period sample in the 4-5 Myr Cep OB3b region published by *Littlefair et al.* (2010) extends into the VLM regime. Taken together with the previously reported samples, there are now more than hundred VLM periods available at ages of 3-5 Myr.

From the period distributions in these very young regions, the following features are noteworthy:

- VLM objects at young ages show a wide range of periods, similar to more massive stars, from a few hours up to at least 2 weeks.
- In all these samples there is a consistent trend of faster rotation towards lower masses. In the ONC, the median period drops from 5 d for  $M > 0.4 M_{\odot}$  to 2.6 d for VLM stars and to 2 d for BDs (*Rodríguez-Ledesma et al.* 2009). As noted by *Cody and Hillenbrand* (2010) and earlier by *Herbst et al.* (2001), this period-mass trend is consistent with specific angular momentum being only weakly dependent on mass below about  $1 M_{\odot}$ . An intriguing case in the context of the period-mass relation is the Cep OB3b region (*Littlefair et al.* 2010). While the same trend is observed, it is much weaker than in the other regions. The VLM stars in Cep OB3b rotate more slowly than in other clusters with similar age. This may be a sign that rotational properties are linked to environmental factors, a possibility that needs further investigation.

- A controversial aspect of the periods in star forming regions is their lower limit. The breakup limit, where centrifugal forces balance gravity, lies between 3 and 5 h at these young ages. *Zapatero Osorio et al.* (2003), *Caballero et al.* (2004), and *Scholz and Eislöffel* (2004a, 2005) report brown dwarf periods that are very close to that limit. On the other hand, the *Cody and Hillenbrand* (2010) sample contains only one period shorter than 14 h, although their sensitivity increases towards shorter periods. Thus, it remains to be confirmed whether some young brown dwarfs indeed rotate close to breakup speed.
- Whether the disk-rotation connection observed for solar-mass and low-mass young stars extends down to the VLM and brown dwarf domains remains unclear. *Cody and Hillenbrand* (2010) found the same period distribution for disk-bearing and diskless VLM stars in the 3 Myr  $\sigma$  Ori cluster while in the 2 Myr ONC *Rodríguez-Ledesma et al.* (2010) find that objects with NIR excess tend to rotate slower than objects without NIR excess in the mass regime between 0.075 and 0.4  $M_{\odot}$ . No such signature is seen in the substellar regime with the possible caveat that many brown dwarf disks show little or no excess emission in the NIR and require MIR data to be clearly detected. Finally, *Mohanty et al.* (2005), *Nguyen et al.* (2009), *Biazzo et al.* (2009), and *Dahm et al.* (2012) report somewhat conflicting results regarding the existence of a disk-rotation connection in the very low mass regime based on  $v \sin i$  measurements of members of 1-5 Myr clusters.

**Pre-main sequence clusters:** For the pre-main sequence age range between 5 and 200 Myr, about 200 VLM periods are now available, a factor of 20 increase compared with 2007. About 80 of them have been measured in IC4665 and NGC2547, two clusters with ages around 40 Myr (*Scholz et al.* 2009; *Irwin et al.* 2008b). Approximately 100 periods are available for VLM objects in NGC2516 ( $\simeq 150$  Myr) from *Irwin et al.* (2007). In addition, a few more VLM periods are contained in the samples for M34 (*Irwin et al.* 2006) and M50 (*Irwin et al.* 2009), although the latter sample might be affected by substantial contamination. Note that in these clusters (as well as in the main-sequence Praesepe cluster discussed below) the number of measured BD periods is very low (probably  $< 5$ ).

The most significant feature in the period distributions in this mass and age regime is the distinctive lack of slow rotators. Essentially all VLM periods measured thus far in these clusters are shorter than 2 d, with a clear preference for periods less than 1 d. The median period is 0.5-0.7 d. The lowest period limit is around 3 h. This preference for fast rotators cannot be attributed to a bias in the period data, for two reasons. First, most of the studies cited above are sensitive to longer periods. Second, *Scholz and Eislöffel* (2004b) demonstrate that the lower envelope of the  $v \sin i$  for Pleiades VLM stars (*Terndrup et al.* 2000) translates

into an upper period limit of only 1-2 d, consistent with the period data.

Compared with the star forming regions, both the upper period limit and the median period drop significantly. As discussed by *Scholz et al.* (2009), this evolution is consistent with angular momentum conservation plus weak rotational braking, but cannot be accommodated by a Skumanich-type wind braking law.

**Main sequence clusters:** For the Praesepe cluster, with an age of 580 Myr a cornerstone for tracing the main-sequence evolution of stars, around 30 rotation periods have been measured for VLM stars (*Scholz and Eislöffel* 2007; *Scholz et al.* 2011). In combination with the samples for more massive stars by *Delorme et al.* (2011) and *Agüeros et al.* (2011), this cluster has now a well defined period sample for FGKM dwarfs (cf. Fig. 1). With one exception, all VLM stars in the Scholz et al. sample have periods less than 2.5 d, with a median around 1 d and a lower limit of 5 h. *Scholz et al.* (2011) compared the Praesepe sample with the pre-main sequence clusters. While the evolution of the lower period limit is consistent with zero or little angular momentum losses between 100 and 600 Myr, the evolution of the upper period limit implies significant rotational braking. In this paper, this is discussed in terms of a mass-dependent spindown on the main sequence. With an exponential spindown law, the braking timescale  $\tau$  is  $\sim 0.5$  Gyr for 0.3  $M_{\odot}$ , but  $> 1$  Gyr for 0.1  $M_{\odot}$ . Thus, wind braking becomes less efficient towards lower masses. Similar to the pre-main sequence clusters, the rotation of brown dwarfs is unexplored in this age regime.

**Field populations:** The largest (in fact, the only large) sample of periods for VLM stars in the field has been published recently by *Irwin et al.* (2011), with 41 periods for stars with masses between the hydrogen burning limit and 0.35  $M_{\odot}$ . A few more periods in this mass domain are available from *Kiraga and Stepien* (2007). Interestingly, the Irwin et al. sample shows a wide spread of periods, from 0.28 d up to 154 d. in stark contrast to the uniformly fast rotation in younger groups of objects. Based on kinematical age estimates, Irwin et al. find that the majority of the oldest objects in the sample (thick disk, halo) are slow rotators, with a median period of 92 d. For comparison, the younger thin disk objects have a median period of 0.7 d. This provides a firm constraint on the spindown timescale of VLM stars, which should be comparable with the thick disk age, i.e., 8-10 Gyr. Similar conclusions were reached by *Delfosse et al.* (1998) and *Mohanty and Basri* (2003) based on  $v \sin i$  measurements.

Brown dwarfs in the field have spectral types of L, T, and Y, and effective temperatures below 2500 K. At these temperatures, magnetic activity as it is known for M dwarfs, is not observed anymore, thus, periodic flux modulations from magnetically induced spots as in VLM stars are not expected. Some L- and T-dwarfs, however, do exhibit persistent periodic variability, which is usually attributed to the presence of a non uniform distribution of atmospheric clouds (see *Radigan et al.* 2012), which again allows for a

measurement of the rotation period. About a dozen of periods for field L- and T-dwarfs are reported in the literature and are most likely the rotation periods (*Bailer-Jones and Mundt* 1999, 2001; *Clarke et al.* 2002; *Koen* 2006; *Lane et al.* 2007; *Artigau et al.* 2009; *Radigan et al.* 2012; *Heinze et al.* 2013). All these periods are shorter than 10 h.

Again it is useful to compare these findings with  $v \sin i$  data. Rotational velocities have been measured for about 100 brown dwarfs by *Mohanty and Basri* (2003), *Zapatero Osorio et al.* (2006), *Reiners and Basri* (2008, 2010), *Blake et al.* (2010), and *Konopacky et al.* (2012). The composite figure by *Konopacky et al.* (2012, their Fig.3) contains about 90 values for L- and 8 for T-dwarfs. From this combined dataset it is clear that essentially all field brown dwarfs are fast rotators with  $v \sin i > 7 \text{ km s}^{-1}$ , corresponding to periods shorter than 17 h, thus confirming the evidence from the smaller sample of periods. The lower limit in  $v \sin i$  increases towards later spectral types, from  $7 \text{ km s}^{-1}$  for early L dwarfs to more than  $20 \text{ km s}^{-1}$  for late L dwarfs and beyond. Because brown dwarfs cool down as they age and thus spectral type is a function of age and mass, these values are difficult to compare with models. However, they strongly suggest that rotational braking becomes extremely inefficient in the substellar domain. Extrapolating from the trend seen in the M dwarfs, the braking timescales for brown dwarfs are expected to be longer than the age of the Universe.

The results of rotational studies of the VLM stars in Praesepe and in the field clearly indicate that the spin-down timescale increases towards lower masses in the VLM regime. There is no clear mass threshold at which the long-term rotational braking ceases to be efficient, as might be expected in a scenario where the dynamo mode switches due to a change in interior structure. The observational data rather suggests that the rotational braking becomes gradually less efficient towards lower masses, until it essentially shuts down for brown dwarfs.

### 2.3 Gyrochronology

By the time low-mass stars reach the ZAMS (100–200 Myr), the observations show clear evidence for two distinct sequences of fast and slow rotators in the mass vs. period plane, presumably tracing the lower and upper envelopes of stellar rotation periods at the ZAMS. Observations in yet older open clusters show a clear convergence in the angular momentum evolution for all FGK dwarfs towards a single, well-defined, and mass-dependent rotation period by the age of the Hyades ( $\sim 600$  Myr, cf. Fig 1).

These patterns—and in particular the observed sequence of slow rotators with stellar mass—have been used as the basis for “gyrochronology” as an empirical tool with which to measure the ages of main-sequence stars (e.g., *Barnes* 2003, 2007; *Mamajek and Hillenbrand* 2008; *Meibom et al.* 2009; *Collier Cameron et al.* 2009; *Delorme et al.* 2011). The method has so far been demonstrated and calibrated for solar-type stars with convective envelopes (i.e., mid-F

to early-M dwarfs), with ages from the ZAMS to the old field population.

In the gyrochronology paradigm, the principal assumptions are that a given star begins its main-sequence rotational evolution with a certain “initial” rotation period on the ZAMS, on either a rapid-rotator sequence (so-called ‘C’ sequence) or a slow-rotator sequence (so-called ‘I’ sequence). All stars on the rapid-rotator sequence evolve onto the slow-rotator sequence on a timescale governed by the convective turnover time of the convective envelope (*Barnes and Kim* 2010). Once on the slow-rotator sequence, the star then spins down in a predictable way with time, thus allowing its age to be inferred from its rotation period.

As discussed by *Epstein and Pinsonneault* (2012), there are limitations to the technique, particularly in the context of very young stars. First, to convert a given star’s observed rotation period into a gyro-age requires assuming the star’s initial rotation period. At older ages, this is not too problematic because the convergence of the gyro-chrones makes the star eventually forget its own initial ZAMS rotation period. However, at ages near the ZAMS, the effect of the (generally unknown) initial period is more important.

More importantly, the technique has not yet been demonstrated or calibrated at ages earlier than the ZAMS. Presumably, the rotational scatter observed at the ZAMS and the relationships between stellar mass and surface rotation period must develop at some stage during the PMS and should be understood in the context of the early angular momentum evolution of individual stars (see Section 4). Interestingly, there is now observational evidence that specific patterns may be emerging during the PMS in the period-mass diagrams, which encode the age of the youngest clusters (*Henderson and Stassun* 2012).

## 3. THE PHYSICAL PROCESSES GOVERNING ANGULAR MOMENTUM EVOLUTION

The evolution of the rotation period and the angular momentum of a forming protostar is determined both by internal and external processes. External processes include all the mechanisms of angular momentum exchange with the surrounding ambient medium, with the accretion disk and the circumstellar outflows in particular. Internal processes determine the angular momentum redistribution throughout the stellar interior. These various processes are discussed in this section.

The upper panel of Figure 2 shows the evolution of the surface rotation rate of a  $1 M_{\odot}$  star, as predicted by *Gallet and Bouvier’s* (2013) models. The blue and red tracks correspond to the upper and lower envelopes of the observed spin distributions, and represent the range of spin evolutions exhibited by the majority of solar-mass stars (cf. Fig. 6). The dotted lines show the evolution of the rotation rate, assuming that the star conserves angular momentum (assuming solid body rotation and structural evolution from *Baraffe et al.* 1998). These angular momentum conserved tracks are shown for a few arbitrary “starting points,”

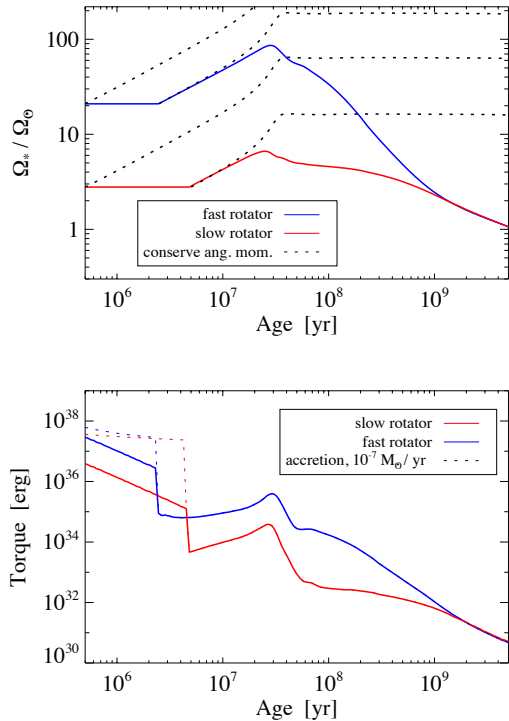


Fig. 2.— *Upper panel:* Angular rotation rate of a  $1 M_{\odot}$  star as a function of age. The red and blue tracks show the evolution of the surface rotation rate from the *Gallet and Bouvier’s* (2013) models, which best reproduce the lower and upper (respectively) range of the observed spin distributions (cf. Fig. 6). The dotted lines show the expected evolution of rotation rate, if the star were to conserve angular momentum, shown at a few different “starting points.” *Lower panel:* The external torque on the star that is required to produce the spin evolution tracks of the upper panel. The red and blue lines show the torque required, assuming only the stellar structural evolution from a model of *Baraffe et al.* (1998) and the (solid-body) spin evolution of the corresponding red and blue lines in the upper panel. The dotted lines show the torque that would be required if the stars were also accreting at a rate of  $10^{-7} M_{\odot} \text{yr}^{-1}$ , during the time when the rotation rate is constant on the upper panel tracks.

at the earliest time shown in the plot and at the time where the rotation rate is no longer constant in time. Assuming angular momentum conservation, the stars are expected to spin up, due to their contraction as they evolve toward the zero-age main sequence (at  $\sim 40$  Myr) and then to have a nearly constant rotation rate on the main sequence (since then the structure changes much more slowly). It is clear from a comparison between the dotted lines and solid lines that the observed evolution is completely inconsistent with angular momentum conservation and instead requires substantial angular momentum loss.

The lower panel of Figure 2 shows the external torque on the star that is necessary to produce the red and blue tracks of the upper panel, assuming solid body rotation. If the star is also accreting from a Keplerian disk, this should in principle result in an additional spin-up torque on the star, given approximately by  $\tau_a \gtrsim \dot{M}_a (GM_* R_*)^{1/2}$ , where  $\dot{M}_a$  is the accretion rate (e.g., *Ghosh and Lamb* 1978; *Matt and Pudritz* 2005b). As a simple quantitative example, the dotted lines in the lower panel show the torque required to produce the gyrotracks of the upper panel, assuming the stars are accreting at a constant rate of  $\dot{M}_a = 10^{-7} M_{\odot} \text{yr}^{-1}$ , during the time when the rotation rate is constant.

It is clear from the figure that the observed evolution of the spin rates of solar-mass stars requires substantial angular momentum loss at nearly all stages, and the required torque is largest at the youngest ages. During the first few Myr of the T Tauri phase, the observed spin-rate distributions do not appear to evolve substantially. The torques required simply to prevent these stars from spinning up, due to contraction, are  $\sim 10^6$  times larger than the torque on the present day Sun. Accreting stars require even larger torques to counteract the additional spin-up effects of accretion, which depends primarily on the accretion rate.

After an age of  $\sim 5$  Myr, and until the stars reach the ZAMS (at  $\sim 40$  Myr), the stars spin up, due to their contraction. Although the surface rotation rates suggest a substantial fraction of their angular momentum is lost during this spin-up phase, the torque is apparently much less than during the first few Myr. This apparent sudden change in the torque suggests a change in the mechanism responsible for angular momentum loss. The fact that a substantial fraction of stars younger than  $\sim 5$  Myr are still accreting suggests that the star-disk interaction may in some way be responsible for the largest torques (*Koenigl* 1991). In this case, the eventual dissipation of the disk (i.e., the cessation of accretion) provides a natural explanation (at least in principle) for the transition to much weaker torques.



### 3.1 Star-disk interaction

Our understanding of the various processes that are involved in the magnetic interaction between the star and its surrounding accretion disk has improved significantly in the last few years (e.g., *Bouvier et al.* 2007). A number of recent results have spurred the development of new models and ideas for angular momentum transport, as well as further development and modification to existing models. In particular, it has been clear for some time that, due to the differential twisting of the magnetic field lines, the stellar magnetic field cannot connect to a very large region in the disk (e.g., *Shu et al.* 1994; *Lovelace et al.* 1995; *Uzdensky et al.* 2002; *Matt and Pudritz* 2005b). In addition, the competition between accretion and diffusion is likely to reduce the magnetic field intensity in the region beyond the corotation radius (*Bardou and Heyvaerts* 1996; *Agapitou and Papanoizou* 2000; *Zanni and Ferreira* 2009). As a consequence, the widespread “disk-locking” paradigm, as proposed in the classical Ghosh & Lamb picture (*Ghosh and Lamb* 1979), has been critically re-examined. Also, it has been realized that the strength of the dipolar components of magnetic fields are generally significantly weaker than the average surface fields, which indicates that the latter is dominated by higher order multipoles (*Gregory et al.* 2012). As the large-scale dipolar field is thought to be the key component for angular momentum loss, mechanisms for extracting angular momentum from the central star are thus required to be even more efficient. These issues have prompted different groups to reconsider and improve various scenarios based on the presence of outflows that could efficiently extract angular momentum from the star-disk system, as schematically illustrated in Figure 3. The key new developments have been (1) the generalization of the X-wind model to multi-polar fields, (2) a renewed exploration of stellar winds as a significant angular momentum loss mechanism, and (3) the recognition that magnetospheric ejections that naturally arise from the star-disk interaction may actually have a significant contribution to the angular momentum transport.

Note that in the following sections we deal with only one specific class of disk winds, namely the X-wind, and neglect other popular models, the “extended disk wind” in particular, presented in *A. Frank et al.’s* chapter. First, in its “standard” formulation (e.g., *Blandford and Payne* 1982; *Ferreira* 1997), an extended disk wind exerts a torque onto the disk without modifying its Keplerian angular momentum distribution. In this respect, such a solution simply allows the disk to accrete and it does not affect the stellar angular momentum evolution. Second, we only discuss models that exploit the stellar magnetic flux. It has been shown (e.g., *Zanni and Ferreira* 2013) that the stellar magnetic field cannot provide enough open flux to the disk to produce a relevant extended disk wind: the latter needs a proper disk field distribution to be powered. Scenarios in which a disk field interacts with the stellar magnetic flux have been proposed (see *Ferreira et al.* 2000) and they de-

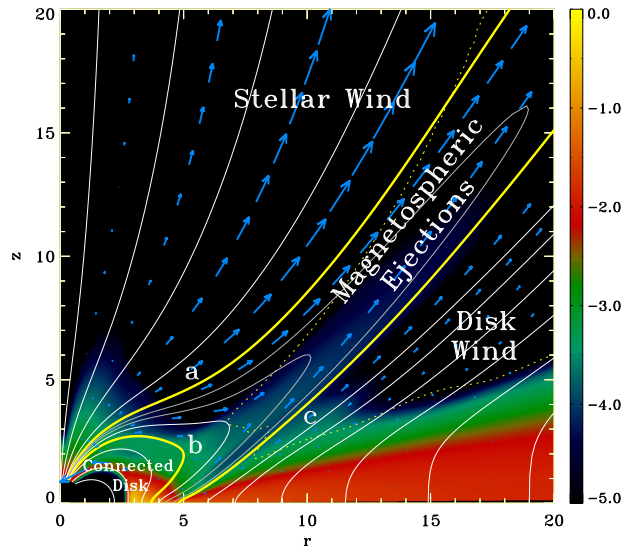


Fig. 3.— Schematic view of the outflows that can be found in a star-disk interacting system. 1) Stellar winds accelerated along the open magnetic flux anchored onto the star; 2) magnetospheric ejections associated with the expansion and reconnection processes of closed magnetic field lines connecting the star and the disk; 3) disk-winds (including X-winds) launched along the open stellar magnetic surfaces threading the disk. From *Zanni and Ferreira* (2013).

serve future investigation.

#### 3.1.1 Accretion driven stellar winds

The idea that stellar winds may be important for removing angular momentum from accreting stars has been around since the first measurements of the rotational properties of young stars (e.g., *Shu et al.* 1988; *Hartmann and Stauffer* 1989). For stars that are actively accreting from a disk, the amount of angular momentum carried onto the star by the disk is proportional to the accretion rate. Stellar winds could be important for counteracting the spin-up effect due to accretion, if the mass outflow rate is a significant fraction ( $\sim 10\%$ ) of the accretion rate (*Hartmann and Stauffer* 1989; *Matt and Pudritz* 2005a). Due to the substantial energy requirements for driving such a wind, *Matt and Pudritz* (2005a) suggested that a fraction of the gravitational potential energy released by accretion (the “accretion power”) may power a stellar wind with sufficiently enhanced mass outflow rates.

The torque from a stellar wind (discussed further below) depends upon many factors, and generally increases with magnetic field strength and also with mass loss rate. Thus, the problem discussed above of having weak dipolar fields can in principle be made up for by having a larger mass loss rate. However, as the mass loss rate approaches a substantial fraction of the mass accretion rate, there will not be enough accretion power to drive the wind. *Matt and Pudritz* (2008b) derived a “hard” upper limit of

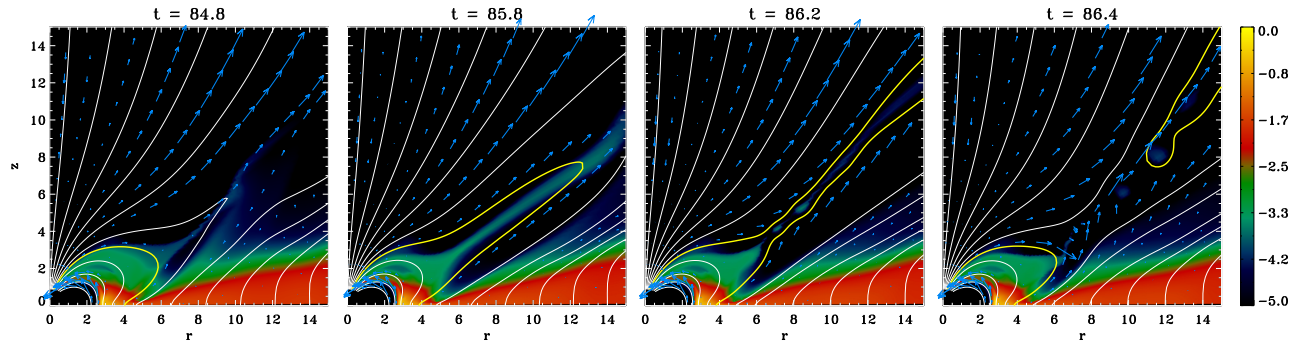


Fig. 4.— Temporal evolution of the periodic inflation/reconnection process associated with magnetospheric ejections. Speed vectors (blue arrows) and magnetic field lines (white lines) are superimposed to logarithmic density maps. The solid yellow line follows the evolution of a single magnetic surface. Time is given in units of the stellar rotation period. From *Zanni and Ferreira (2013)*.

$\dot{M}_{wind}/\dot{M}_{acc} \lesssim 60\%$ . By considering that the accretion power must be shared between (at least) the stellar wind and the observed accretion diagnostics (e.g., the UV excess luminosity), *Zanni and Ferreira (2011)* made a quantitative comparison between the predictions of accretion-powered stellar winds and an observed sample of accreting stars, to test whether there was enough accretion power available to drive a wind capable of removing the accreted angular momentum. The range of observational uncertainties in quantities such as the UV excess and dipolar magnetic field strength was sufficient to span the range of possibilities from having enough accretion power to not having enough accretion power. However, this work demonstrated again that accretion-powered stellar winds need substantial large-scale magnetic fields in order to be efficient, and the strength of the observed fields are (within uncertainties) near the minimum required strengths (*Gregory et al. 2012*).

Even if there is enough accretion power to drive a wind, there is still a question of whether or how accretion power may transfer to the open field regions of a star and drive a wind. Based on calculations of the emission properties and cooling times of the gas, *Matt and Pudritz (2007)* ruled out solar-like, hot coronal winds for mass loss rates greater than  $\sim 10^{-11} M_{\odot}/\text{yr}$  for “typical” T Tauri stars of  $\sim 0.5 M_{\odot}$ . They concluded that more massive winds would be colder (colder than  $\sim 10,000\text{K}$ ) and thus must be driven by something other than thermal pressure, such as Alfvén waves (*Decampli 1981*). Taking a “first principles” approach and adopting a simplified, 1-D approach, *Cranmer (2008, 2009)* developed models whereby the energy associated with variable accretion drove MHD waves that traveled from the region of accretion on the star to the polar regions where it led to enhanced MHD wave activity and drove stellar wind. Those models typically reached mass loss rates that were equal or less than a few percent of the accretion rate. These values appear to be on the low end of what is needed for significant angular momentum loss for most observed systems. Further theoretical work is needed to explore how accretion power may transfer to a stellar wind.

### 3.1.2 Magnetospheric ejections

Magnetospheric ejections (MEs) are expected to arise because of the expansion and subsequent reconnection of the closed magnetospheric field lines connecting the star to the disk (*Hayashi et al. 1996; Goodson et al. 1999; Zanni and Ferreira 2013*). The inflation process is the result of the star-disk differential rotation and the consequent build-up of toroidal magnetic field pressure. This is the same phenomenon that bounds the size of the closed magnetosphere and limits the efficiency of the *Ghosh and Lamb (1979)* mechanism. Initially, MEs are launched along magnetic field lines which still connect the star with the disk so that they can exchange mass, energy and angular momentum both with the star and the disk. On a larger spatial scale, the MEs disconnect from the central region of the disk-star system in a magnetic reconnection event and propagate ballistically as magnetized plasmoids. Because of magnetic reconnection, the inner magnetic surfaces close again and the process repeats periodically (see Fig. 4). This phenomenon is likely to be related to the “conical winds” simulated by *Romanova et al. (2009)*.

MEs contribute to control the stellar rotation period in two ways (*Zanni and Ferreira 2013*). First, they extract angular momentum from the disk close to the truncation region so that the spin-up accretion torque is sensibly reduced. This effect closely resembles the action of an X-wind (see next subsection), which represents the limit solution capable of extracting all the angular momentum carried by the accretion flow. Second, if the ejected plasma rotates slower than the star, the MEs can extract angular momentum directly from the star thanks to a differential rotation effect. In such a situation, MEs are powered by both the stellar and the disk rotation, as in a huge magnetic slingshot. In agreement with other popular scenarios (*Koenigl 1991; Ostriker and Shu 1995*), the spin-down torque exerted by the MEs can balance the accretion torque when the disk is truncated close to the corotation radius. In a propeller phase (see, e.g., *Ustyugova et al. 2006; D’Angelo and Spruit 2011*), when the truncation radius gets even closer to corotation, the spin-down torque can even balance the spin-

up due to contraction.

Despite these first encouraging results, various issues remain. The MEs phenomenon is based on a charge and discharge process whose periodicity and efficiency depend on magnetic reconnection events that are controlled by numerical diffusion only in the solutions proposed by *Zanni and Ferreira* (2013). In order to produce an efficient spin-down torque, this scenario requires a rather strong kG dipolar field component, which has been only occasionally observed in classical T Tauri stars (e.g., *Donati et al.* 2008, 2010b). In the propeller regime, which provides the most efficient spin-down torque, the accretion rate becomes intermittent on a dynamical timescale, corresponding to a few rotation periods of the star. Even though this effect is enhanced by the axial symmetry of the models, there is as yet no observational evidence for such a behavior.

### 3.1.3 X-Winds

The X-wind model<sup>1</sup> invokes the interaction of the stellar magnetosphere with the surrounding disk to explain the slow spin rates of accreting T Tauri stars, well below break-up, within a single theoretical framework, via the central concept of *trapped flux*. In steady-state, the basic picture is as follows (see Fig. 5): all the stellar magnetic flux initially threading the entire disk is trapped within a narrow annulus (the X-region) at the disk inner edge. The X-region straddles the corotation radius  $R_X$  (where the disk Keplerian angular velocity,  $\Omega_X = \sqrt{GM_*/R_X^3}$ , equals the stellar angular velocity,  $\Omega_*$ ;  $R_X$  lies near, but exterior to, the inner-edge), a feature known as disk-locking. The resulting dominance of the magnetic pressure over gas within the X-region makes the entire annulus rotate as a solid body at the corotation angular velocity  $\Omega_X = \Omega_*$ . Consequently, disk material slightly interior to  $R_X$  rotates at sub-Keplerian velocities, allowing it to climb efficiently onto field lines that bow sufficiently inwards and accrete onto the star; conversely, material within the X-region but slightly exterior to  $R_X$  rotates at super-Keplerian velocities, enabling it to ascend field lines that bend sufficiently outwards and escape in a wind. The magnetic torques associated with the accretion funnels transfer excess specific angular momentum (excess relative to the amount already residing on the star) from the infalling gas to the disk material at the foot-points of the funnel flow field lines in the inner parts of the X-region, which tends to push this material outwards. Conversely, the magnetic torques in the wind cause the outflowing gas to gain angular momentum at the expense of the disk material connected to it by field lines rooted in the outer parts of the X-region, pushing this material inwards. The pinch due to this outward push on the inside, and inward push on the outside, of the X-region is what keeps the flux trapped within it, and truncates the disk at the inner-edge in the first place. The net result is a transfer of angular

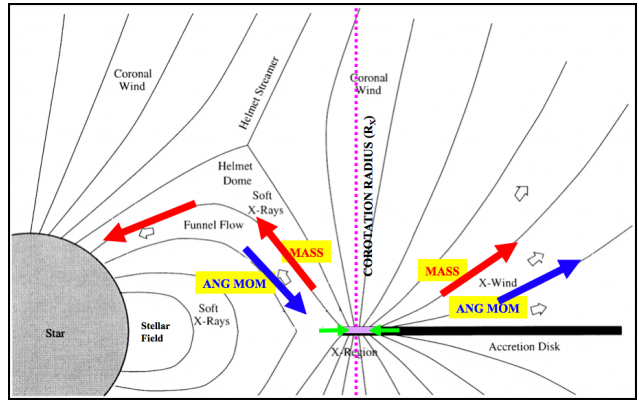


Fig. 5.— Schematic of steady-state X-wind model. *Black thick line* in the equatorial plane is the truncated disk; *black solid curves* show the magnetic field; *purple dotted line* shows the co-rotation radius  $R_X$ ; *purple thick horizontal line* shows the X-region. Red and blue arrows show the direction of mass and angular momentum transport respectively: interior to  $R_X$ , material flows from the X-region onto the star in a funnel flow along field lines that bow sufficiently inwards, and the excess angular momentum in this gas flows back into the X-region via magnetic stresses; exterior to  $R_X$ , material flows out of the X-region in a wind, along field lines that bow sufficiently outwards, and carries away with it angular momentum from the X-region. *Green arrows* show the pinching of gas in the X-region due to the angular momentum transport, which truncates the disk at the inner edge and keeps magnetic flux trapped in the X-region.

momentum from the accreting gas to the wind, allowing the star to remain slowly rotating.

The X-wind accretion model was originally formulated assuming a dipole stellar field (*Ostriker and Shu* 1995). However, detailed spectropolarimetric reconstructions of the stellar surface field point to more complex field configurations (e.g., *Donati et al.* 2010a, 2011). In view of this, and noting that the basic idea of flux trapping, as outlined above, does not depend on the precise field geometry, *Mohanty and Shu* (2008) generalized the X-wind accretion model to arbitrary multipole fields. The fundamental relationship in this case, for a star of mass  $M_*$ , radius  $R_*$  and angular velocity  $\Omega_*$ , is

$$F_h R_*^2 \bar{B}_h = \bar{\beta} f^{1/2} (GM_* \dot{M}_D / \Omega_*)^{1/2} \quad (1).$$

Here  $F_h$  is the fraction of the surface area  $2\pi R_*^2$  of one hemisphere of the stellar surface (either above or below the equatorial plane) covered by accretion hot spots with mean field strength  $\bar{B}_h$ ;  $\bar{\beta}$  is a dimensionless, inverse mass-loading parameter, that measures the ratio of magnetic field to mass flux; and  $f$  is the fraction of the total disk accretion rate  $\dot{M}_D$  that flows into the wind (so  $1-f$  is the fraction that accretes onto the star). Equation (1) encapsulates the concept of flux trapping: it relates the amount of observed flux in hot spots on the left-hand side (which equals

<sup>1</sup>Other types of outflows are considered in *Frank et al.*'s chapter

the amount of trapped flux in the X-region that is loaded with infalling gas) to independently observable quantities on the right-hand side, without any assumptions about the specific geometry of the stellar field that ultimately drives the funnel flow.

There is now some significant evidence for the generalized X-wind model. First, surveys of classical T Tauri stars in Taurus and NGC 2264 strongly support the correlation  $F_h R_*^2 \propto (GM_* \dot{M}_D / \Omega_*)^{1/2}$ , predicted by equation (1) if  $\bar{B}_h$  can be assumed constant, an assumption admittedly open to debate (*Johns-Krull and Gafford 2002; Cauley et al. 2012*). Second, in two stars with directly measured  $\bar{B}_h$  from spectropolarimetric data, as well as estimates of  $F_h$ ,  $\dot{M}$  and stellar parameters (V2129 Oph and BP Tau; *Donati et al. 2007, 2008*, respectively), *Mohanty and Shu (2008)* find that equation (1) (with some simplistic assumptions about  $\beta$  and  $f$ ; see also below) produces excellent agreement with the observed  $\bar{B}_h F_h$ ; they also find that numerical models incorporating the mix of multipole components observed on these stars give  $F_h$ ,  $\bar{B}_h$  and hot spot latitudes consistent with the data. More generally, there is substantial evidence that disks are involved in regulating the angular momentum of the central star, but evidence for disk-locking (disk truncation close to the corotation radius  $R_X$ ), as specifically proposed by X-wind theory, is as yet inconclusive; more detailed studies of statistical significant samples are required (see Section 2.1).

Support for the X-wind model from numerical simulations has so far been mixed. Using dipole stellar fields, *Romanova et al. (2007)* have obtained winds and funnel flows consistent with the theory over extended durations, but many others (e.g., *Long et al. 2007, 2008*) have failed. It is noteworthy in this regard that, in the presence of finite resistivity  $\eta$ , the flux trapping that is key to the X-wind model requires that field diffusion out of the X-region be offset by fluid advection of field into it. This in turn demands that  $\eta/\nu \ll 1$ , where  $\nu$  is the disk viscosity (*Shu et al. 2007*). *Romanova et al. (2007)* explicitly show that this condition is critical for attaining an X-type magnetic configuration, while other simulations typically have  $\nu \sim \eta$  instead.

Finally, as an ideal-MHD, steady-state, axisymmetric semi-analytic model with a stellar field aligned with the rotation axis, X-wind theory clearly has limitations. For instance, with non-zero resistivity, reconnection events can lead to episodic outbursts; similarly, changes in the stellar field or disk accretion rate, and tilted and/or non-axisymmetric fields can all lead to temporally varying phenomena, as indeed observed in classical T Tauri stars (e.g., *Alencar et al. 2012*). X-wind theory can at best represent only the time-averaged behaviour of an intrinsically time-variable system; numerical simulations are essential for quantitatively exploring these issues in detail (e.g., *Romanova et al. 2011; Long et al. 2011*). Similarly, in the idealized model, the X-region shrinks to a mathematical point, and how the infinitesimal  $\nu$  and  $\eta$  then load field lines is not answerable within the theory, leading to somewhat ad hoc estimates for  $f$  and  $\beta$  (see *Mohanty and Shu*

*2008; Cai et al. 2008*). An associated question is what the appropriate ratio  $\eta/\nu$  is for realistic disks. Global numerical simulations of the magneto-rotational instability (MRI), with non-zero magnetic flux, are vital to shed light on these issues (see *Shu et al. 2007*).

### 3.2 Stellar winds

Most stars spend the majority of their lives in isolation, in a sense that after  $\sim 10$  Myr of age, they are no longer accreting material and most do not possess companions that are within reach of their magnetospheres nor close enough for significant tidal interactions. For isolated stars, the only available way of losing substantial angular momentum is by losing mass. It has been known for a long time that low-mass stars (those with substantial convective envelopes) are magnetically active and spin-down via stellar winds (e.g., *Parker 1958; Kraft 1967; Skumanich 1972; Soderblom 1983*). The coupling of the magnetic field with the wind can make the angular momentum loss very efficient, in a sense that the fractional loss of angular momentum can be a few orders of magnitude larger than the fractional amount of mass lost (e.g., *Schatzman 1962; Weber and Davis 1967; Mestel 1968; Reiners et al. 2009*).

In order to calculate the amount of angular momentum loss due to magnetized stellar winds, the theory generally assumes the conditions of ideal MHD and a steady-state flow. These assumptions are acceptable for characterizing the average, global wind properties, as needed to understand the long-timescale evolution of stellar rotation. In this case, the torque on the star can generally be expressed as (e.g., *Matt et al. 2012a*)

$$T_w = K (2GM_*)^{-m} R_*^{5m+2} \dot{M}_w^{1-2m} B_*^{4m} \Omega_*, \quad (1)$$

where  $M_*$  and  $R_*$  are the stellar mass and radius,  $\dot{M}_w$  the mass loss rate,  $B_*$  the stellar magnetic field, and  $\Omega_*$  the stellar angular velocity.  $K$  and  $m$  are dimensionless numbers that depend upon the interaction between the accelerating flow and rotating magnetic field.

Until recently, most models for computing the angular momentum evolution of stars (discussed below, see Section 4) have used the stellar wind torque formulation of *Kawaler (1988, based on Mestel 1984)*, which is equivalent to equation (1) with a value of  $m = 0.5$  and fitting the constant  $K$  in order to match the present day solar rotation rate. This formulation is convenient because, for  $m = 0.5$ , the stellar wind torque is independent of the mass loss rate (see eq. (1)). For given stellar parameters, one only needs to specify how the surface magnetic field strength depends upon rotation rate, discussed further below.

However, *Kawaler's* formulation relies upon a 1D approach and adopts simple power-law relationships for how the magnetic field strength and the wind velocity vary with distance from the star. *Matt and Pudritz (2008a)* pointed out that these assumptions are not generally valid in multi-dimensional winds and that numerical simulations

are needed to accurately and self-consistently determine the values of  $K$  and  $m$ . Using 2D (axisymmetric) numerical MHD simulations, *Matt and Pudritz (2008a)* and *Matt et al. (2012a)* computed steady-state solutions for coronal (thermally driven) winds in the case of stars with a dipolar magnetic field aligned with the rotation axis. Using parameter studies to determine how the torque varies, *Matt et al. (2012a)* found

$$m \approx 0.2177 \quad K \approx 6.20 [1 + (f/0.0716)^2]^{-m}, \quad (2)$$

where  $f$  is the stellar rotation rate expressed as a fraction of breakup (Keplerian rate at the stellar surface),  $f^2 \equiv \Omega_*^2 R_*^3 (GM_*)^{-1}$ . Note that the dimensionless factor  $K$  now contains a dependence on the stellar spin rate (in addition to that appearing in eq. (1)), and it is nearly constant when the star rotates slower than a few percent of breakup speed.

The formulation of equations (1) and (2) is derived from simulations with fixed assumptions about the wind driving (e.g., coronal temperature) and a particular (dipolar) field geometry on the stellar surface. Thus, further work is needed to determine how the torque depends upon the wind driving properties<sup>2</sup> and varies for more complex magnetic geometries. However, this is the most-dynamically self-consistent stellar wind torque formulation to date.

After adopting equation (2), it is clear that the torque in equation (1) depends upon both the surface magnetic field strength and the mass loss rate. To specify the magnetic field strength, most spin evolution models adopt the relationship suggested by *Kawaler (1988)*,  $B_* \propto \Omega_*^a R_*^{-2}$ . The value of  $a$  is usually taken to be unity for slow rotators, but above some critical rotation rate of approximately  $10 \Omega_\odot$  for solar-type stars, the magnetic field is taken to be independent of rotation rate by setting  $a = 0$ . The so-called “dynamo saturation” above some critical velocity is observationally supported both by direct magnetic field measurements (e.g., *Reiners et al. 2009*) and activity proxies (e.g., *Wright et al. 2011*).

Recently, *Reiners and Mohanty (2012)* pointed out that both observations of magnetic fields (e.g., *Saar 1996; Reiners et al. 2009*) and dynamo theory (e.g., *Durney and Stenflo 1972; Chabrier and Küker 2006*) were more consistent with a dynamo relationship following  $B_* \propto \Omega_*^a$ —that is, the average magnetic field *strength* goes as some power of  $\Omega$ , instead of the magnetic *flux* (as in the Kawaler formulation). This has important implications for the dependence of the torque on the mass (and radius) of the star. Furthermore, *Reiners and Mohanty (2012)* derived a new torque formulations, based on similar assumptions to Kawaler’s, arriving at the equivalent of equation (1), with  $m = 2/3$ . Although this value of  $m$  is inconsistent with the MHD simulation results discussed above, *Reiners and Mohanty (2012)* demon-

strated that, in order to simultaneously explain the observed spin evolution of both solar mass and very low mass stars, the stellar wind torque must depend much more strongly on the stellar mass (and radius) than the Kawaler formulation.

To calculate the torque, we also need to know how the mass loss rate depends on stellar properties. Due to the relatively low loss rates of non-accreting sun-like and low mass stars, observational detections and measurements are difficult. So far, most of what we know is based on approximately a dozen measurements by *Wood et al. (2002, 2005)*, which suggest that the mass loss rates vary nearly linearly with the X-ray luminosity, up to a threshold X-ray flux, above which the mass loss rates saturate. More recently, *Cranmer and Saar (2011)* have developed a theoretical framework for predicting the mass loss rates of low mass stars, based upon the propagation and dissipation of Alfvén waves (and see *Suzuki et al. 2012*). The models of *Cranmer and Saar (2011)* and *Suzuki et al. (2012)* compute the mass loss rate as a function of stellar parameters in a way that is self-consistent with the scaling of magnetic field strength with stellar rotation rate (including both saturated and non-saturated regimes). These models can now be used, in conjunction with equations (1) and (2) to compute the stellar wind torque during most of the lifetime of an isolated, low-mass star.

As another means of probing the mass loss rates, *Aarnio et al. (2012)* used an observed correlation between coronal mass ejections and X-ray flares, together with the observed flare rate distributions derived from T Tauri stars in Orion (*Albacete Colombo et al. 2007*), to infer mass loss rates due to coronal mass ejections alone. *Drake et al. (2013)* presented a similar analysis for main sequence stars. Furthermore, *Aarnio et al. (2012)* explored how coronal mass ejections may influence the angular momentum evolution of pre-main-sequence stars. They concluded that they are not likely to be important during the accretion phase or during early contraction, but they could potentially be important after  $\sim 10$  Myr. Although there are a number of uncertainties associated with estimating CME mass loss rates from observed X-ray properties, this an interesting area for further study.

### 3.3 Internal processes

As angular momentum is removed from the stellar surface by external processes, such as star-disk interaction and stellar winds, the evolution of the surface rotation rate depends in part on how angular momentum is transported in the stellar interior. Two limiting cases are i) solid-body rotation, where it is assumed that angular momentum loss at the stellar surface is instantaneously redistributed throughout the whole stellar interior, i.e., the star has uniform rotation from the center to the surface, and ii) complete core-envelope decoupling, where only the outer convective zone is spun down while the inner radiative core accelerates as it develops during the PMS, thus yielding a large velocity gradient at the core-envelope interface. Presumably, the ac-

<sup>2</sup>*Ud-Doula et al. (2009)* reported  $m \approx 0.25$ , derived from their simulations of massive star winds, driven by radiation, rather than thermal pressure. This suggests that the value of  $m$  does not strongly vary with the wind driving properties.

tual rotational profile of solar-type and low mass stars lies between these two extremes. Until recently, only the internal rotation profile of the Sun was known (*Schou et al.* 1998). Thanks to Kepler data, internal rotation has now been measured for a number of giant stars evolving off the main sequence from the seismic analysis of mixed gravity and pressure modes (e.g., *Deheuvels et al.* 2012). The internal rotation profile of PMS stars and of field main sequence stars is, however, still largely unconstrained by the observations.

A number of physical processes act to redistribute angular momentum throughout the stellar interior. These include various classes of hydrodynamical instabilities (e.g., *Decressin et al.* 2009; *Pinsonneault* 2010; *Lagarde et al.* 2012; *Eggenberger et al.* 2012), magnetic fields (e.g., *Denissenkov and Pinsonneault* 2007; *Spada et al.* 2010; *Strugarek et al.* 2011), and gravity waves (*Charbonnel et al.* 2013; *Mathis* 2013), all of which may be at work during PMS evolution. At the time of writing this review, only few of the current models describing the angular momentum evolution of young stars include these processes from first principles (e.g., *Denissenkov et al.* 2010; *Turck-Chièze et al.* 2010; *Charbonnel et al.* 2013; *Marques et al.* 2013; *Mathis* 2013) and highlight the need for additional physics to account for the observations. Pending fully-consistent physical models, most current modeling efforts adopt empirical prescriptions for core-envelope angular momentum exchange as discussed below.

#### 4. ANGULAR MOMENTUM EVOLUTION MODELS

In an attempt to account for the observational results described in Section 2, most recent models of angular momentum evolution rest on the 3 main physical processes described in Section 3, namely: star-disk interaction, wind braking and angular momentum redistribution in the stellar interior. Each of these processes is included in the models in a variety of ways, as described below:

- *Star-disk interaction:* only few recent models attempt to provide a physical description of the angular momentum exchange taking place between the star and its accretion disk. For instance, *Matt et al.* (2012b) computed the evolution of the torque exerted by accretion-powered stellar winds onto the central star during the early accreting PMS phase. Another example, is the work of *Gallet and Zanni (in prep.)*, who combined the action of accretion-driven winds and magnetospheric ejections to account for the nearly constant angular velocity of young PMS stars in spite of accretion and contraction. Both models require dipolar magnetic field components of about 1-2 kG, i.e., on the high side of the observed range of magnetic field strength in young stars (*Donati and Landstreet* 2009; *Donati et al.* 2013; *Gregory et al.* 2012). Most other models, however, merely assume constant angular velocity for the cen-

tral star as long as it accretes from its disk (as originally proposed by *Koenigl* 1991), with the disk lifetime being a free parameter in these models (e.g., *Irwin et al.* 2007, 2008a; *Bouvier* 2008; *Irwin and Bouvier* 2009; *Denissenkov* 2010; *Reiners and Mohanty* 2012; *Gallet and Bouvier* 2013).

- *Wind braking:* up to a few years ago, most models used *Kawaler's* (1988) semi-empirical prescription, with the addition of saturation at high velocities (as originally suggested by *Stauffer and Hartmann* 1987), to estimate the angular momentum loss rate due to magnetized winds (see, e.g., *Bouvier et al.* 1997; *Krishnamurthi et al.* 1997; *Sills et al.* 2000). Recently, more physically-sounded braking laws have been proposed. *Reiners and Mohanty* (2012) revised *Kawaler's* prescription on the basis of a better understanding of dynamo-generated magnetic fields, while *Matt et al.* (2012a) used 2D MHD simulations to derive a semi-analytical formulation of the external torque exerted on the stellar surface by stellar winds. The latter result has been used in the angular momentum evolution models developed for solar-type stars by *Gallet and Bouvier* (2013), who also provide a detailed comparison between the various braking laws.
- *Internal angular momentum transport:* while some models do include various types of angular momentum transport processes (e.g., *Denissenkov et al.* 2010; *Turck-Chièze et al.* 2010; *Charbonnel et al.* 2013; *Marques et al.* 2013), the most popular class of models so far rely on the simplifying assumption that the star consists of a radiative core and a convective envelope that are both in solid-body rotation but at different rates. In these so-called double-zone models, angular momentum is exchanged between the core and the envelope at a rate set by the core-envelope coupling timescale, a free parameter of this class of models (e.g., *Irwin et al.* 2007; *Bouvier* 2008; *Irwin et al.* 2009; *Denissenkov* 2010; *Spada et al.* 2011). When dealing with fully convective interiors, whether PMS stars on their Hayashi track or very-low mass stars, models usually assume solid-body rotation throughout the star.

We illustrate below how these classes of models account for the observed spin rate evolution of solar-type stars, low-mass and very low-mass stars, and brown dwarfs.

##### 4.1 Solar-type stars

Figure 6 (from *Gallet and Bouvier* 2013) shows the observed and modeled angular momentum evolution of solar-type stars in the mass range 0.9-1.1  $M_{\odot}$ , from the start of the PMS at 1 Myr to the age of the Sun. The rotational

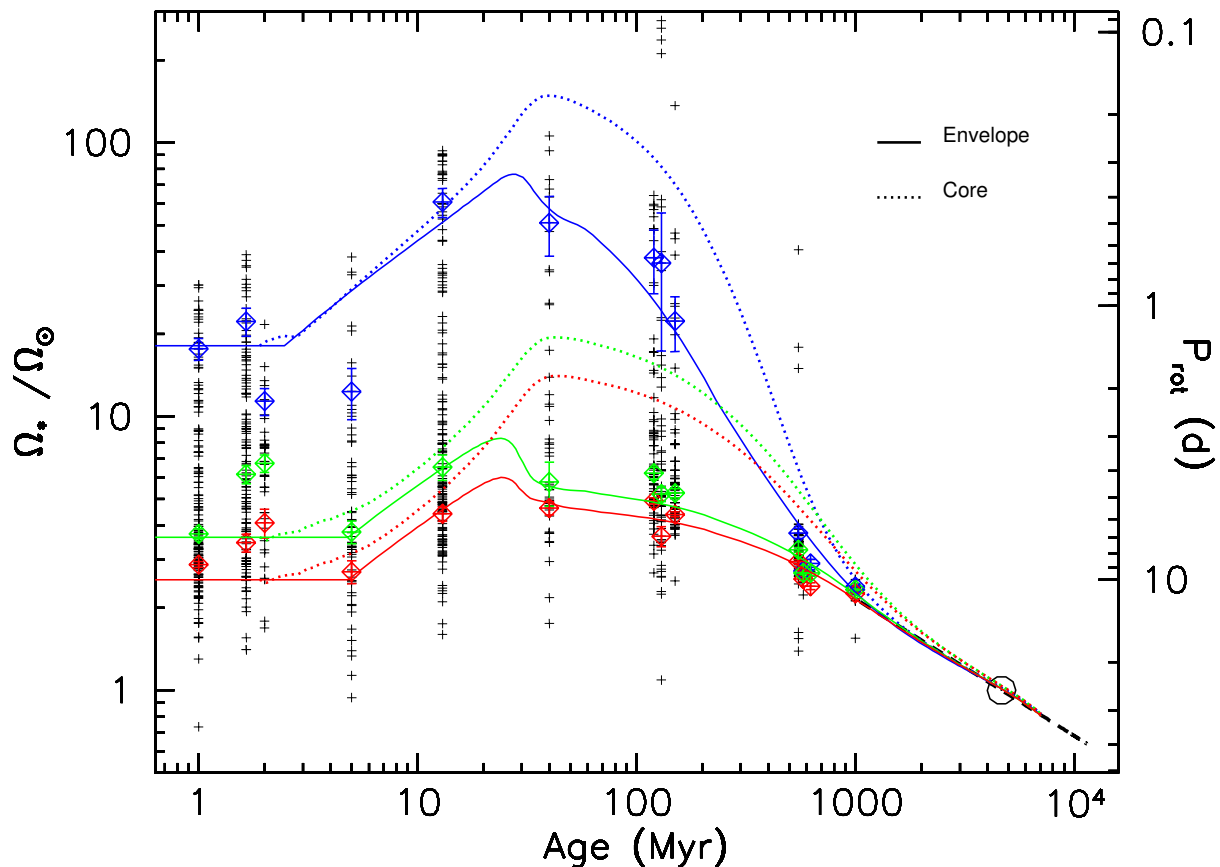


Fig. 6.— The rotational angular velocity of solar-type stars is plotted as a function of age. The left y-axis is labelled with angular velocity scaled to the angular velocity of the present Sun while the right y-axis is labelled with rotational period in days. On the x-axis the age is given in Myr. *Observations:* The black crosses shown at various age steps are the rotational periods measured for solar-type stars in star forming regions and young open clusters over the age range 1 Myr–1 Gyr. The red, green, and blue diamonds represent the 25, 50, and 90th percentiles of the observed rotational distributions, respectively. The open circle at 4.56 Gyr is the angular velocity of the present Sun. *Models:* The angular velocity of the convective envelope (solid line) and of the radiative core (dashed lines) is shown as a function of time for slow (red), median (green), and fast (blue) rotator models, with initial periods of 10, 7, and 1.4 days, respectively. The dashed black line at the age of the Sun illustrates the asymptotic Skumanich relationship,  $\Omega \propto t^{-1/2}$ . From *Gallet and Bouvier (2013)*.

distributions of solar-type stars are shown at various time steps corresponding to the age of the star forming regions and young open clusters to which they belong (cf. Fig 1). Three models are shown, which start with initial periods of 10, 7, and 1.4 days, corresponding to slow, median, and fast rotators, respectively. The models assume constant angular velocity during the star-disk interaction phase in the early PMS, and implement the *Matt et al. (2012a)* wind braking prescription, as well as core-envelope decoupling. The free parameters of the models are the initial periods, chosen to fit the rotational distributions of the earliest clusters, the star-disk interaction timescale  $\tau_d$  during which the angular velocity is held constant at its initial value, the core-envelope coupling timescale  $\tau_{ce}$ , and the calibration constant  $K_W$  for wind-driven angular momentum losses. The latter is fixed by the requirement to fit the Sun’s angular velocity at the Sun’s age. These parameters are varied until a reasonable

agreement with observations is obtained. In this case, the slow, median, and fast rotator models aim at reproducing the 25, 50, and 90<sup>th</sup> percentiles of the observed rotational distributions and their evolution from the early PMS to the age of the Sun.

This class of models provide a number of insights into the physical processes at work. The star-disk interaction lasts for a few Myr in the early PMS, and possibly longer for slow rotators ( $\tau_d \simeq 5$  Myr) than for fast ones ( $\tau_d \simeq 2.5$  Myr). As the disk dissipates, the star begins to spin up as it contracts towards the ZAMS. The models then suggest much longer core-envelope coupling timescales for slow rotators ( $\tau_{ce} \simeq 30$  Myr) than for fast ones ( $\tau_{ce} \simeq 12$  Myr). Hence, on their approach to the ZAMS, only the outer convective envelope of slow rotators is spun down while their radiative core remains in rapid rotation. They consequently develop large angular velocity gradients at the interface be-

tween the radiative core and the convective envelope on the ZAMS and, indeed, most of their initial angular momentum is then hidden in their radiative core (cf. *Gallet and Bouvier 2013*)<sup>3</sup>. As stars evolve on the early MS, wind braking eventually leads to the convergence of rotation rates for all models by an age of  $\simeq 1$  Gyr. This is due to the strong dependency of the braking rate onto the angular velocity: faster rotators are braked more efficiently than slow ones. Also, the early-MS spin evolution of slow rotators is flatter than that of fast rotators, in part because the angular momentum hidden in the radiative core at the ZAMS resurfaces on a timescale of a few 0.1 Gyr on the early MS. These models illustrate the strikingly different rotational histories solar-type stars may experience prior to about 1 Gyr, depending mostly on their initial period and disk lifetime. In turn, the specific rotational history a young star undergoes may have a long-lasting impact on its properties, such as lithium content, even long after rotational convergence is completed (e.g., *Bouvier 2008; Randich 2010*).

These models describe the spin evolution of isolated stars while many cool stars belong to multiple stellar systems (cf. *Duchêne and Kraus 2013*). For short period binaries ( $P_{orb} \leq 12$  days), tidal interaction enforces synchronization between the orbital and rotational periods (*Zahn 1977*) and the spin evolution of the components of such systems will clearly differ from that of single stars (*Zahn and Bouchet 1989*). However, the fraction of such tight, synchronized systems among solar-type stars is low, of order of 3% (*Raghavan et al. 2010*), so that tidal effects are unlikely to play a major role in the angular momentum evolution of most cool stars. Another potentially important factor is the occurrence of planetary systems (e.g., *Mayor et al. 2011; Bonfils et al. 2013*). The frequency of hot Jupiters, i.e., massive planets close enough to their host star to have a significant tidal or magnetospheric influence (cf. *Dobbs-Dixon et al. 2004; Lanza 2010; Cohen et al. 2010*), is quite low, amounting to a mere 1% around FGK stars (e.g., *Wright et al. 2012*). However, there is mounting evidence that the formation of planetary systems is quite a dynamic process, with gravitational interactions taking place between forming and/or migrating planets (*Albrecht et al. 2012*, see also the chapters by *Davies et al.* and *Baruteau et al.*), which may lead to planet scattering and even planet engulfment by the host star. The impact of such catastrophic events onto the angular momentum evolution of planet-bearing stars has been investigated by *Bolmont et al. (2012)* who showed it could significantly modify the instantaneous spin rate of planet host stars both during the PMS and on the main sequence.

<sup>3</sup> Note that the effect of hiding some angular momentum in the radiative core would “smooth out” the torques shown in Fig. 2, where solid-body rotation was assumed. Namely, the ZAMS torques will be slightly less and the post-ZAMS will be slightly larger to an age of  $\sim 1$  Gyr, due to the effects of differential rotation and core-envelope decoupling

## 4.2 Very low-mass stars

Models similar to those described above for solar-type stars have been shown to apply to lower mass stars, at least down to the fully convective boundary ( $\simeq 0.3 M_{\odot}$ ), with the core-envelope coupling timescale apparently lengthening as the convective envelope thickens (e.g., *Irwin et al. 2008b*). In the fully convective regime, i.e., below  $0.3 M_{\odot}$ , models ought to be simpler as the core-envelope decoupling assumption becomes irrelevant and uniform rotation is usually assumed throughout the star. Yet, the rotational evolution of very low-mass stars actually appears more complex than that of their more massive counterparts and still challenges current models. Figure 7 (from *Irwin et al. 2011*) shows that disk locking still seems to be required for VLM stars in order to account for their slowly evolving rotational period distributions during the first few Myr of PMS evolution. Yet, as discussed above (see Section 2.2), the evidence for a disk-rotation connection in young VLM stars is, at best, controversial. Equally problematic, the rotational period distribution of field M-dwarfs appears to be bimodal, with pronounced peaks at fast (0.2-10 d) and slow (30-150 d) rotation (*Irwin et al. 2011*). Most of the slow rotators appear to be thick disk members, i.e., they are on average older than the fast ones that are kinematically associated to the thin disk, and the apparent bimodality could thus simply result from a longer spin down timescale for VLM stars, of order of a few Gyr, as advocated by *Reiners and Mohanty (2012)* and *McQuillan et al. (2013)*.

However, as shown in Figure 7, this bimodality may not be easily explained for field stars at an age of several Gyr. Indeed, contrary to solar-type stars whose rotational scatter decreases from the ZAMS to the late-MS (cf. Fig. 6), the distribution of spin rates of VLM stars widens from the ZAMS to later ages. The large dispersion of rotation rates observed at late ages for VLM stars thus requires drastically different model assumptions. Specifically, for a given model mass ( $0.25 M_{\odot}$  in Fig. 7), the calibration of the wind-driven angular momentum loss rate has to differ by one order of magnitude between slow and fast rotators (*Irwin et al. 2011*). Why does a fraction of VLM stars remain fast rotators over nearly 10 Gyr while another fraction is slowed down on a timescale of only a few Gyr is currently unclear. A promising direction to better understand the rotational evolution of VLM stars is the recently reported evidence for a bimodality in their magnetic properties. Based on spectropolarimetric measurements of the magnetic topology of late M dwarfs obtained by *Morin et al. (2010)*, *Gastine et al. (2013)* have suggested that a bistable dynamo operates in fully convective stars, which results in two contrasting magnetic topologies: either strong axisymmetric dipolar fields or weak multipolar fields. Whether the different magnetic topologies encountered among M dwarfs is at the origin of their rotational dispersion at late ages remains to be assessed.



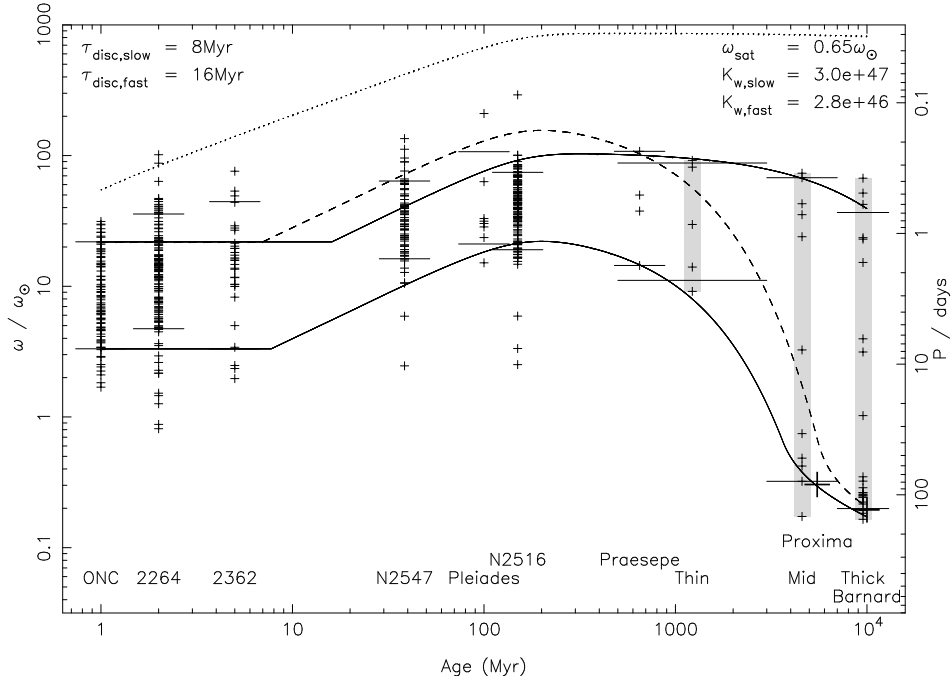


Fig. 7.— The rotational angular velocity of very low-mass stars ( $0.1\text{-}0.35 M_{\odot}$ ) is plotted as a function of age. The left y-axis is labelled with angular velocity scaled to the angular velocity of the present Sun while the right y-axis is labelled with rotational period in days. On the x-axis the age is given in Myr. *Observations:* The black crosses shown at various age steps are the rotational periods measured for very low-mass stars in star forming regions, young open clusters, and in the field over the age range 1 Myr-10 Gyr. Short horizontal lines show the 10th and 90th percentiles of the angular velocity distributions at a given age, used to characterize the slow and fast rotators, respectively. *Models:* The solid curves show rotational evolution models for  $0.25 M_{\odot}$  stars, fit to the percentiles, with the upper curve for the rapid rotators (with parameters  $\tau_{d,fast}$  and  $K_{W,fast}$ ) and the lower curve for the slow rotators (with parameters  $\tau_{d,slow}$  and  $K_{W,slow}$ ). Note the factor of 10 difference between  $K_{W,fast}$  and  $K_{W,slow}$ . The dashed curve shows the result for the rapid rotators if the wind parameter  $K_{W,fast}$  is assumed to be the same as for the slow rotators rather than allowing it to vary. The dotted curve shows the break-up limit. From *Irwin et al. (2011)*.

### 4.3 Brown dwarfs

Figure 8 illustrates the current rotational data and models for brown dwarfs (BDs) from 1 Myr to the field substellar population. As discussed in Section 2.2 above, substellar objects are characterized by fast rotation from their young age throughout their whole evolution, with a median period of about 2 d at 1 Myr and 3-4 h at 1 Gyr. Somewhat controversial evidence for disk locking has been reported among young BDs (see Sect. 2.2 above), although sensitive mid-IR surveys are still needed for large samples in order to better characterize the disk frequency. Figure 8 shows models computed with and without angular momentum losses from (sub)stellar winds. The evolution of substellar rotational distributions in the first few Myr is consistent with either no or moderate disk locking, as previously advocated by *Lamm et al. (2005)*. At an age of a few Myr, the observed rotation rates suggest substellar objects experience little an-

gular momentum loss on this timescale. By an age of a few Gyr, however, some angular momentum loss has occurred. The best fit to the observational constraints is obtained with models featuring an angular momentum loss rate for BDs that is about 10,000 times weaker than that assumed for solar-type stars (cf. Fig. 6). Whether the inefficient rotational braking of brown dwarf results from a peculiar magnetic topology, their predominantly neutral atmospheres, or some other cause is currently unclear.

### 4.4 Summary

Current models of the spin evolution of low-mass stars appear to converge towards the following consensus:

- At all masses, the initial distribution of angular momentum exhibit a large dispersion that must reflect some process operating during the core collapse

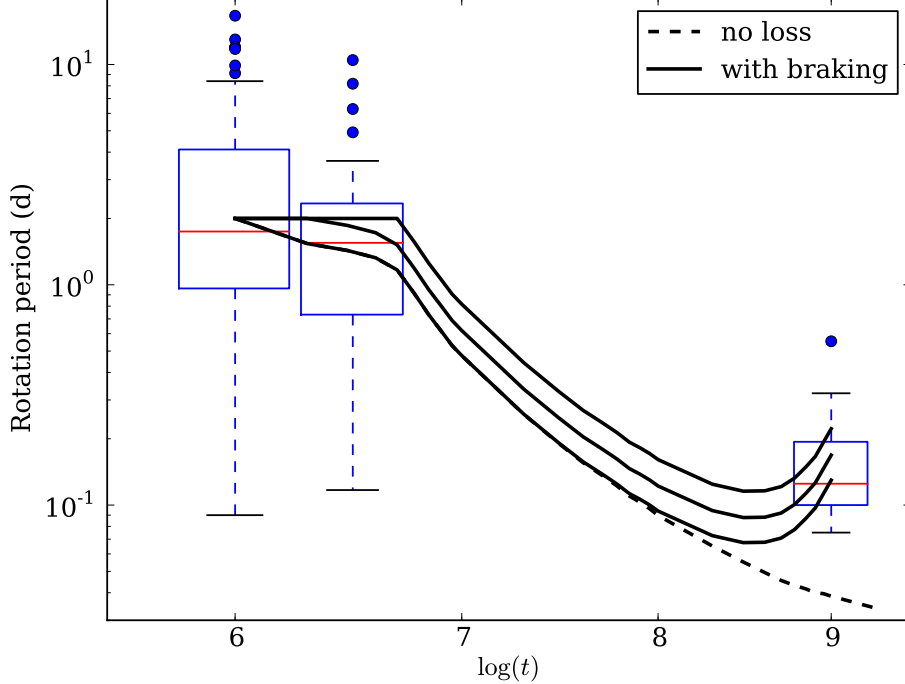


Fig. 8.— Boxplot showing rotation periods for brown dwarfs as a function of age. The plot contains periods for  $\sim 1$  Myr (ONC *Rodríguez-Ledesma et al. 2009*), for  $\sim 3$  Myr (*Cody and Hillenbrand 2010*; *Scholz and Eislöffel 2004a, 2005*; *Bailer-Jones and Mundt 2001*; *Zapatero Osorio et al. 2003*; *Caballero et al. 2004*), and for the field population, for convenience plotted at an age of 1 Gyr although individual ages may vary (*Bailer-Jones and Mundt 2001*; *Clarke et al. 2002*; *Koen 2006*; *Lane et al. 2007*; *Artigau et al. 2009*; *Radigan et al. 2012*; *Girardin et al. 2013*; *Gillon et al. 2013*; *Heinze et al. 2013*). *Red line*: median; *box*: lower and upper quartile; *'whiskers'*: range of datapoints within  $1.5\times$  (75% - 25%) range. Outliers outside that range are plotted as individual datapoints. Note that a few more brown dwarf periods have been measured at other ages, not shown here due to the small sample sizes. The dashed line illustrates evolution models without angular momentum loss. The 3 solid lines correspond to models including saturated angular momentum losses and disk locking phases lasting for 1, 2, and 5 Myr, respectively, with object radii taken from the  $0.05 M_{\odot}$  BT-Settl evolutionary models of *Allard et al. (2011)*. The best fit to the current observational constraints is obtained by assuming an angular momentum loss rate for brown dwarfs that is  $\sim 10,000$  times weaker than that used for solar-type stars shown in Fig. 6.

and/or the embedded protostellar stage. Current models do not solve for this initial rotational scatter but adopt it as initial conditions.

- Some disk related process is required at least for solar-type and low mass stars during the first few Myr in order to account for their hardly evolving rotational period distributions during the early PMS. Whether this process is still instrumental in the VLM and sub-stellar regimes remains to be assessed. The disk lifetimes required by angular momentum evolution models are consistent with those empirically derived from the evolution of IR excess in young stars (e.g., *Bell et al. 2013*).
- Rotational braking due to magnetized winds is strongly mass dependent, being much less efficient at very low masses. At a given mass, angular momentum loss must also scale with the spin rate in

order to account for the rotational convergence of solar-type and low-mass stars on a timescale of a few 0.1 Gyr. The spin down timescale from the ZAMS increases towards lower mass stars (from  $\sim 0.1$  Gyr at  $1 M_{\odot}$  to  $\sim 1$  Gyr at  $0.3 M_{\odot}$ , and  $\geq 10$  Gyr at  $\leq 0.1 M_{\odot}$ ), but once completed, the rotational convergence usually occurs at a lower spin rate for lower mass stars (*McQuillan et al. 2013*).

- Some form of core-envelope decoupling must be introduced in the models in order to simultaneously account for the specific spin evolution of initially slow and fast rotators. The empirically-derived core-envelope coupling timescale is found to be longer in slow rotators than in fast ones at a given mass, thus providing some hints at the underlying physical process responsible for angular momentum transport in stellar interiors.

## 5. CONCLUSION

In the last few years, we have reached a stage where the rotational evolution of cool stars and brown dwarfs is relatively well constrained by the observations. Additional rotational period measurements for homogeneous and coeval populations are still required to fill a few age and mass gaps, e.g., old ( $\geq 1$  Gyr) field dwarfs and ZAMS cluster (0.1–0.5 Gyr) brown dwarfs, so as to provide a complete picture of the spin evolution of stars and substellar objects. The physical description of the mechanisms that dictate the spin evolution of cool stars has also tremendously progressed over the last years, with the exploration of new processes and the refinement of prior ones. Yet, the slow rotation rates of young stars still remain very much of a challenge to these models. A better characterization of the critical quantities involved in the star-disk interaction and in stellar winds, such as the stellar magnetic field intensity and topology, the mass accretion rate onto the star, and the amount of mass loss a star experiences during its lifetime, is sorely needed in order to progress on these issues. In spite of these limitations, the semi-empirical angular momentum evolution models developed to date appear to grasp some of the major trends of the observed spin evolution of cool stars and brown dwarfs. Undoubtedly, the main area of progress to be expected in the next few years lies in the improved physical modeling of these processes.

*Acknowledgments* The authors would like to dedicate this contribution to the memory of Jean Heyvaerts who passed away the week before PPVI. JB acknowledges the grant ANR 2011 Blanc SIMI5-6 020 01 Toupies: Towards understanding the spin evolution of stars ([http://ipag.osug.fr/Anr\\_Toupies/](http://ipag.osug.fr/Anr_Toupies/)). KGS and SPM acknowledge the USA National Science Foundation (NSF) grant AST-0808072. KGS also acknowledges NSF grant AST-0849736. SM acknowledges the support of the UK STFC grant ST/H00307X/1, and many invaluable discussions with F. Shu and A. Reiners. We thank Florian Gallet and Jonathan Irwin for providing Fig.6 and Fig.7 of this review chapter, respectively. We are indebted to the many authors who have provided us with the data used to build Fig.1 of this review chapter.

## REFERENCES

- Aarnio A. N., Matt S. P., and Stassun K. G. (2012) *Astrophys. J.*, 760, 9.
- Affer L., Micela G., Favata F. et al. (2012) *Mon. Not. R. Astron. Soc.*, 424, 11.
- Affer L., Micela G., Favata F. et al. (2013) *Mon. Not. R. Astron. Soc.*, 430, 1433.
- Agapitou V. and Pappalouizou J. C. B. (2000) *Mon. Not. R. Astron. Soc.*, 317, 273.
- Agüeros M. A., Covey K. R., Lemonias J. J. et al. (2011) *Astrophys. J.*, 740, 110.
- Albacete Colombo J. F., Caramazza M., Flaccomio E. et al. (2007) *Astron. Astrophys.*, 474, 495.
- Albrecht S., Winn J. N., Johnson J. A. et al. (2012) *Astrophys. J.*, 757, 18.
- Alencar S. H. P., Bouvier J., Walter F. M. et al. (2012) *Astron. Astrophys.*, 541, A116.
- Alencar S. H. P., Teixeira P. S., Guimarães M. M. et al. (2010) *Astron. Astrophys.*, 519, A88.
- Allard F., Homeier D., and Freytag B. (2011) in: *16th Cambridge Workshop on Cool Stars, Stellar Systems, and the Sun*, vol. 448 of *Astronomical Society of the Pacific Conference Series*, (edited by C. Johns-Krull, M. K. Browning, and A. A. West), p. 91.
- Artemenko S. A., Grankin K. N., and Petrov P. P. (2012) *Astronomy Letters*, 38, 783.
- Artigau É., Bouchard S., Doyon R. et al. (2009) *Astrophys. J.*, 701, 1534.
- Bailer-Jones C. A. L. and Mundt R. (1999) *Astron. Astrophys.*, 348, 800.
- Bailer-Jones C. A. L. and Mundt R. (2001) *Astron. Astrophys.*, 367, 218.
- Baraffe I., Chabrier G., Allard F. et al. (1998) *Astron. Astrophys.*, 337, 403.
- Bardou A. and Heyvaerts J. (1996) *Astron. Astrophys.*, 307, 1009.
- Barnes S. A. (2003) *Astrophys. J.*, 586, 464.
- Barnes S. A. (2007) *Astrophys. J.*, 669, 1167.
- Barnes S. A. and Kim Y.-C. (2010) *Astrophys. J.*, 721, 675.
- Bell C. P. M., Naylor T., Mayne N. J. et al. (2013) *Mon. Not. R. Astron. Soc.*, 434, 806.
- Biazzo K., Melo C. H. F., Pasquini L. et al. (2009) *Astron. Astrophys.*, 508, 1301.
- Blake C. H., Charbonneau D., and White R. J. (2010) *Astrophys. J.*, 723, 684.
- Blandford R. D. and Payne D. G. (1982) *Mon. Not. R. Astron. Soc.*, 199, 883.
- Bolmont E., Raymond S. N., Leconte J. et al. (2012) *Astron. Astrophys.*, 544, A124.
- Bonfils X., Delfosse X., Udry S. et al. (2013) *Astron. Astrophys.*, 549, A109.
- Bouvier J. (2008) *Astron. Astrophys.*, 489, L53.
- Bouvier J., Alencar S. H. P., Harries T. J. et al. (2007) *Protostars and Planets V*, pp. 479–494.
- Bouvier J., Forestini M., and Allain S. (1997) *Astron. Astrophys.*, 326, 1023.
- Caballero J. A., Béjar V. J. S., Rebolo R. et al. (2004) *Astron. Astrophys.*, 424, 857.
- Cai M. J., Shang H., Lin H.-H. et al. (2008) *Astrophys. J.*, 672, 489.
- Carr J. S. (2007) in: *IAU Symposium*, vol. 243 of *IAU Symposium*, (edited by J. Bouvier and I. Appenzeller), pp. 135–146.
- Cauley P. W., Johns-Krull C. M., Hamilton C. M. et al. (2012) *Astrophys. J.*, 756, 68.
- Chabrier G. and Küker M. (2006) *Astron. Astrophys.*, 446, 1027.
- Charbonnel C., Decressin T., Amard L. et al. (2013) *Astron. Astrophys.*, 554, A40.
- Cieza L. and Baliber N. (2007) *Astrophys. J.*, 671, 605.
- Clarke F. J., Tinney C. G., and Covey K. R. (2002) *Mon. Not. R. Astron. Soc.*, 332, 361.
- Cody A. M. and Hillenbrand L. A. (2010) *Astrophys. J. Suppl.*, 191, 389.
- Cohen O., Drake J. J., Kashyap V. L. et al. (2010) *Astrophys. J. Lett.*, 723, L64.

- Collier Cameron A., Davidson V. A., Hebb L. et al. (2009) *Mon. Not. R. Astron. Soc.*, 400, 451.
- Cranmer S. R. (2008) *Astrophys. J.*, 689, 316.
- Cranmer S. R. (2009) *Astrophys. J.*, 706, 824.
- Cranmer S. R. and Saar S. H. (2011) *Astrophys. J.*, 741, 54.
- Dahm S. E., Slesnick C. L., and White R. J. (2012) *Astrophys. J.*, 745, 56.
- D'Angelo C. R. and Spruit H. C. (2011) *Mon. Not. R. Astron. Soc.*, 416, 893.
- Decampli W. M. (1981) *Astrophys. J.*, 244, 124.
- Decressin T., Mathis S., Palacios A. et al. (2009) *Astron. Astrophys.*, 495, 271.
- Deheuveils S., García R. A., Chaplin W. J. et al. (2012) *Astrophys. J.*, 756, 19.
- Delfosse X., Forveille T., Perrier C. et al. (1998) *Astron. Astrophys.*, 331, 581.
- Delorme P., Collier Cameron A., Hebb L. et al. (2011) *Mon. Not. R. Astron. Soc.*, 413, 2218.
- Denissenkov P. A. (2010) *Astrophys. J.*, 719, 28.
- Denissenkov P. A. and Pinsonneault M. (2007) *Astrophys. J.*, 655, 1157.
- Denissenkov P. A., Pinsonneault M., Terndrup D. M. et al. (2010) *Astrophys. J.*, 716, 1269.
- Dobbs-Dixon I., Lin D. N. C., and Mardling R. A. (2004) *Astrophys. J.*, 610, 464.
- Donati J., Gregory S., Alencar S. et al. (2013) *ArXiv e-prints*.
- Donati J.-F., Gregory S. G., Montmerle T. et al. (2011) *Mon. Not. R. Astron. Soc.*, 417, 1747.
- Donati J.-F., Jardine M. M., Gregory S. G. et al. (2007) *Mon. Not. R. Astron. Soc.*, 380, 1297.
- Donati J.-F., Jardine M. M., Gregory S. G. et al. (2008) *Mon. Not. R. Astron. Soc.*, 386, 1234.
- Donati J.-F. and Landstreet J. D. (2009) *Annu. Rev. Astron. Astrophys.*, 47, 333.
- Donati J.-F., Skelly M. B., Bouvier J. et al. (2010a) *Mon. Not. R. Astron. Soc.*, 402, 1426.
- Donati J.-F., Skelly M. B., Bouvier J. et al. (2010b) *Mon. Not. R. Astron. Soc.*, 409, 1347.
- Drake J. J., Cohen O., Yashiro S. et al. (2013) *eprint arXiv*, 1302, 1136.
- Duchêne G. and Kraus A. (2013) *Annu. Rev. Astron. Astrophys.*, 51, 269.
- Durney B. R. and Stenflo J. O. (1972) *Astrophys. Space Sci.*, 15, 307.
- Eggenberger P., Montalbán J., and Miglio A. (2012) *Astron. Astrophys.*, 544, L4.
- Epstein C. R. and Pinsonneault M. H. (2012) *ArXiv e-prints*.
- Ferreira J. (1997) *Astron. Astrophys.*, 319, 340.
- Ferreira J., Pelletier G., and Appl S. (2000) *Mon. Not. R. Astron. Soc.*, 312, 387.
- Gallet F. and Bouvier J. (2013) *Astron. Astrophys.*, 556, A36.
- Gastine T., Morin J., Duarte L. et al. (2013) *Astron. Astrophys.*, 549, L5.
- Ghosh P. and Lamb F. K. (1978) *Astrophys. J. Lett.*, 223, L83.
- Ghosh P. and Lamb F. K. (1979) *Astrophys. J.*, 234, 296.
- Gillon M., Triaud A. H. M. J., Jehin E. et al. (2013) *Astron. Astrophys.*, 555, L5.
- Girardin F., Artigau É., and Doyon R. (2013) *Astrophys. J.*, 767, 61.
- Goodson A. P., Böhm K.-H., and Winglee R. M. (1999) *Astrophys. J.*, 524, 142.
- Grankin K. N. (2013) *Astronomy Letters*, 39, 251.
- Gregory S. G., Donati J.-F., Morin J. et al. (2012) *Astrophys. J.*, 755, 97.
- Harrison T. E., Coughlin J. L., Ule N. M. et al. (2012) *Astron. J.*, 143, 4.
- Hartman J. D., Bakos G. Á., Kovács G. et al. (2010) *Mon. Not. R. Astron. Soc.*, 408, 475.
- Hartman J. D., Gaudi B. S., Pinsonneault M. H. et al. (2009) *Astrophys. J.*, 691, 342.
- Hartmann L. and Stauffer J. R. (1989) *Astron. J.*, 97, 873.
- Hayashi M. R., Shibata K., and Matsumoto R. (1996) *Astrophys. J. Lett.*, 468, L37.
- Heinze A. N., Metchev S., Apai D. et al. (2013) *Astrophys. J.*, 767, 173.
- Henderson C. B. and Stassun K. G. (2012) *Astrophys. J.*, 747, 51.
- Herbst W., Bailer-Jones C. A. L., and Mundt R. (2001) *Astrophys. J. Lett.*, 554, L197.
- Herbst W., Bailer-Jones C. A. L., Mundt R. et al. (2002) *Astron. Astrophys.*, 396, 513.
- Herbst W., Eislöffel J., Mundt R. et al. (2007) *Protostars and Planets V*, pp. 297–311.
- Irwin J., Aigrain S., Bouvier J. et al. (2009) *Mon. Not. R. Astron. Soc.*, 392, 1456.
- Irwin J., Aigrain S., Hodgkin S. et al. (2006) *Mon. Not. R. Astron. Soc.*, 370, 954.
- Irwin J., Berta Z. K., Burke C. J. et al. (2011) *Astrophys. J.*, 727, 56.
- Irwin J. and Bouvier J. (2009) in: *IAU Symposium*, vol. 258 of *IAU Symposium*, (edited by E. E. Mamajek, D. R. Soderblom, and R. F. G. Wyse), pp. 363–374.
- Irwin J., Hodgkin S., Aigrain S. et al. (2007) *Mon. Not. R. Astron. Soc.*, 377, 741.
- Irwin J., Hodgkin S., Aigrain S. et al. (2008a) *Mon. Not. R. Astron. Soc.*, 384, 675.
- Irwin J., Hodgkin S., Aigrain S. et al. (2008b) *Mon. Not. R. Astron. Soc.*, 383, 1588.
- Johns-Krull C. M. and Gafford A. D. (2002) *Astrophys. J.*, 573, 685.
- Kawaler S. D. (1988) *Astrophys. J.*, 333, 236.
- Kiraga M. and Stepien K. (2007) *Acta Astron.*, 57, 149.
- Koen C. (2006) *Mon. Not. R. Astron. Soc.*, 367, 1735.
- Koenigl A. (1991) *Astrophys. J. Lett.*, 370, L39.
- Konopacky Q. M., Ghez A. M., Fabrycky D. C. et al. (2012) *Astrophys. J.*, 750, 79.
- Kraft R. P. (1967) *Astrophys. J.*, 150, 551.
- Krishnamurthi A., Pinsonneault M. H., Barnes S. et al. (1997) *Astrophys. J.*, 480, 303.
- Lagarde N., Decressin T., Charbonnel C. et al. (2012) *Astron. Astrophys.*, 543, A108.
- Lamm M. H., Mundt R., Bailer-Jones C. A. L. et al. (2005) *Astron. Astrophys.*, 430, 1005.
- Lane C., Hallinan G., Zavala R. T. et al. (2007) *Astrophys. J. Lett.*, 668, L163.
- Lanza A. F. (2010) *Astron. Astrophys.*, 512, A77.
- Le Blanc T. S., Covey K. R., and Stassun K. G. (2011) *Astron. J.*, 142, 55.
- Littlefair S. P., Naylor T., Mayne N. J. et al. (2010) *Mon. Not. R. Astron. Soc.*, 403, 545.
- Long M., Romanova M. M., Kulkarni A. K. et al. (2011) *Mon. Not. R. Astron. Soc.*, 413, 1061.
- Long M., Romanova M. M., and Lovelace R. V. E. (2007) *Mon. Not. R. Astron. Soc.*, 374, 436.
- Long M., Romanova M. M., and Lovelace R. V. E. (2008) *Mon.*

- Not. R. Astron. Soc.*, 386, 1274.
- Lovelace R. V. E., Romanova M. M., and Bisnovaty-Kogan G. S. (1995) *Mon. Not. R. Astron. Soc.*, 275, 244.
- Mamajek E. E. and Hillenbrand L. A. (2008) *Astrophys. J.*, 687, 1264.
- Marques J. P., Goupil M. J., Lebreton Y. et al. (2013) *Astron. Astrophys.*, 549, A74.
- Mathis S. (2013) in: *Lecture Notes in Physics, Berlin Springer Verlag*, vol. 865 of *Lecture Notes in Physics, Berlin Springer Verlag*, (edited by M. Goupil, K. Belkacem, C. Neiner, F. Lignières, and J. J. Green), p. 23.
- Matt S. and Pudritz R. E. (2005a) *Astrophys. J. Lett.*, 632, L135.
- Matt S. and Pudritz R. E. (2005b) *Mon. Not. R. Astron. Soc.*, 356, 167.
- Matt S. and Pudritz R. E. (2007) in: *IAU Symposium*, vol. 243 of *IAU Symposium*, (edited by J. Bouvier and I. Appenzeller), pp. 299–306.
- Matt S. and Pudritz R. E. (2008a) *Astrophys. J.*, 678, 1109.
- Matt S. and Pudritz R. E. (2008b) *Astrophys. J.*, 681, 391.
- Matt S. P., MacGregor K. B., Pinsonneault M. H. et al. (2012a) *Astrophys. J. Lett.*, 754, L26.
- Matt S. P., Pinzón G., Greene T. P. et al. (2012b) *Astrophys. J.*, 745, 101.
- Mayor M., Marmier M., Lovis C. et al. (2011) *ArXiv e-prints*.
- McQuillan A., Aigrain S., and Mazeh T. (2013) *Mon. Not. R. Astron. Soc.*, 432, 1203.
- Meibom S., Barnes S. A., Latham D. W. et al. (2011a) *Astrophys. J. Lett.*, 733, L9.
- Meibom S., Mathieu R. D., and Stassun K. G. (2009) *Astrophys. J.*, 695, 679.
- Meibom S., Mathieu R. D., Stassun K. G. et al. (2011b) *Astrophys. J.*, 733, 115.
- Messina S., Desidera S., Lanzafame A. C. et al. (2011) *Astron. Astrophys.*, 532, A10.
- Messina S., Desidera S., Turatto M. et al. (2010) *Astron. Astrophys.*, 520, A15.
- Mestel L. (1968) *Mon. Not. R. Astron. Soc.*, 138, 359.
- Mestel L. (1984) *3rd Cambridge Workshop on Cool Stars, Stellar Systems, and the Sun*, 193, 49.
- Mohanty S. and Basri G. (2003) *Astrophys. J.*, 583, 451.
- Mohanty S., Jayawardhana R., and Basri G. (2005) *Mem. Soc. Astron. Italiana*, 76, 303.
- Mohanty S. and Shu F. H. (2008) *Astrophys. J.*, 687, 1323.
- Moraux E., Artemenko S., Bouvier J. et al. (2013) *ArXiv e-prints*.
- Morin J., Donati J.-F., Petit P. et al. (2010) *Mon. Not. R. Astron. Soc.*, 407, 2269.
- Nguyen D. C., Jayawardhana R., van Kerkwijk M. H. et al. (2009) *Astrophys. J.*, 695, 1648.
- Nielsen M. B., Gizon L., Schunker H. et al. (2013) *Astron. Astrophys.*, 557, L10.
- Ostriker E. C. and Shu F. H. (1995) *Astrophys. J.*, 447, 813.
- Parker E. N. (1958) *Astrophys. J.*, 128, 664.
- Percy J. R., Grynko S., Seneviratne R. et al. (2010) *PASP*, 122, 753.
- Pinsonneault M. H. (2010) in: *IAU Symposium*, vol. 268 of *IAU Symposium*, (edited by C. Charbonnel, M. Tosi, F. Primas, and C. Chiappini), pp. 375–380.
- Pinte C., Ménard F., Berger J. P. et al. (2008) *Astrophys. J. Lett.*, 673, L63.
- Radigan J., Jayawardhana R., Lafrenière D. et al. (2012) *Astrophys. J.*, 750, 105.
- Raghavan D., McAlister H. A., Henry T. J. et al. (2010) *Astrophys. J. Suppl.*, 190, 1.
- Randich S. (2010) in: *IAU Symposium*, vol. 268 of *IAU Symposium*, (edited by C. Charbonnel, M. Tosi, F. Primas, and C. Chiappini), pp. 275–283.
- Rebull L. M., Wolff S. C., and Strom S. E. (2004) *Astron. J.*, 127, 1029.
- Reiners A. and Basri G. (2008) *Astrophys. J.*, 684, 1390.
- Reiners A. and Basri G. (2010) *Astrophys. J.*, 710, 924.
- Reiners A., Basri G., and Browning M. (2009) *Astrophys. J.*, 692, 538.
- Reiners A. and Mohanty S. (2012) *Astrophys. J.*, 746, 43.
- Reiners A., Scholz A., Eislöffel J. et al. (2009) in: *15th Cambridge Workshop on Cool Stars, Stellar Systems, and the Sun*, vol. 1094 of *American Institute of Physics Conference Series*, (edited by E. Stempels), pp. 250–257.
- Rodríguez-Ledesma M. V., Mundt R., and Eislöffel J. (2009) *Astron. Astrophys.*, 502, 883.
- Rodríguez-Ledesma M. V., Mundt R., and Eislöffel J. (2010) *Astron. Astrophys.*, 515, A13.
- Romanova M. M., Long M., Kulkarni A. K. et al. (2007) in: *IAU Symposium*, vol. 243 of *IAU Symposium*, (edited by J. Bouvier and I. Appenzeller), pp. 277–290.
- Romanova M. M., Long M., Lamb F. K. et al. (2011) *Mon. Not. R. Astron. Soc.*, 411, 915.
- Romanova M. M., Ustyugova G. V., Koldoba A. V. et al. (2009) *Mon. Not. R. Astron. Soc.*, 399, 1802.
- Saar S. H. (1996) in: *Stellar Surface Structure*, vol. 176 of *IAU Symposium*, (edited by K. G. Strassmeier and J. L. Linsky), p. 237.
- Schatzman E. (1962) *Annales d'Astrophysique*, 25, 18.
- Scholz A. and Eislöffel J. (2004a) *Astron. Astrophys.*, 419, 249.
- Scholz A. and Eislöffel J. (2004b) *Astron. Astrophys.*, 421, 259.
- Scholz A. and Eislöffel J. (2005) *Astron. Astrophys.*, 429, 1007.
- Scholz A. and Eislöffel J. (2007) *Mon. Not. R. Astron. Soc.*, 381, 1638.
- Scholz A., Eislöffel J., and Mundt R. (2009) *Mon. Not. R. Astron. Soc.*, 400, 1548.
- Scholz A., Irwin J., Bouvier J. et al. (2011) *Mon. Not. R. Astron. Soc.*, 413, 2595.
- Schou J., Antia H. M., Basu S. et al. (1998) *Astrophys. J.*, 505, 390.
- Shu F., Najita J., Ostriker E. et al. (1994) *Astrophys. J.*, 429, 781.
- Shu F. H., Galli D., Lizano S. et al. (2007) *Astrophys. J.*, 665, 535.
- Shu F. H., Lizano S., Ruden S. P. et al. (1988) *Astrophys. J. Lett.*, 328, L19.
- Sills A., Pinsonneault M. H., and Terndrup D. M. (2000) *Astrophys. J.*, 534, 335.
- Skumanich A. (1972) *Astrophys. J.*, 171, 565.
- Soderblom D. R. (1983) *Astrophys. J. Suppl.*, 53, 1.
- Spada F., Lanzafame A. C., and Lanza A. F. (2010) *Mon. Not. R. Astron. Soc.*, 404, 641.
- Spada F., Lanzafame A. C., Lanza A. F. et al. (2011) *Mon. Not. R. Astron. Soc.*, 416, 447.
- Stauffer J. R. and Hartmann L. W. (1987) *Astrophys. J.*, 318, 337.
- Strugarek A., Brun A. S., and Zahn J.-P. (2011) *Astron. Astrophys.*, 532, A34.
- Sukhbold T. and Howell S. B. (2009) *PASP*, 121, 1188.
- Suzuki T. K., Imada S., Kataoka R. et al. (2012) *eprint arXiv*, 1212, 6713.
- Terndrup D. M., Stauffer J. R., Pinsonneault M. H. et al. (2000) *Astron. J.*, 119, 1303.
- Turck-Chièze S., Palacios A., Marques J. P. et al. (2010) *Astro-*

- phys. J.*, 715, 1539.
- Ud-Doula A., Owocki S. P., and Townsend R. H. D. (2009) *Mon. Not. R. Astron. Soc.*, 392, 1022.
- Ustyugova G. V., Koldoba A. V., Romanova M. M. et al. (2006) *Astrophys. J.*, 646, 304.
- Uzdensky D. A., Königl A., and Litwin C. (2002) *Astrophys. J.*, 565, 1191.
- Weber E. J. and Davis L. (1967) *Astrophys. J.*, 148, 217.
- Wood B. E., Müller H.-R., Zank G. P. et al. (2002) *Astrophys. J.*, 574, 412.
- Wood B. E., Müller H.-R., Zank G. P. et al. (2005) *Astrophys. J.*, 628, L143.
- Wright J. T., Marcy G. W., Howard A. W. et al. (2012) *Astrophys. J.*, 753, 160.
- Wright N. J., Drake J. J., Mamajek E. E. et al. (2011) *Astrophys. J.*, 743, 48.
- Xiao H. Y., Covey K. R., Rebull L. et al. (2012) *Astrophys. J. Suppl.*, 202, 7.
- Zahn J.-P. (1977) *Astron. Astrophys.*, 57, 383.
- Zahn J.-P. and Bouchet L. (1989) *Astron. Astrophys.*, 223, 112.
- Zanni C. and Ferreira J. (2009) *Astron. Astrophys.*, 508, 1117.
- Zanni C. and Ferreira J. (2011) *Astrophys. J. Lett.*, 727, L22.
- Zanni C. and Ferreira J. (2013) *Astron. Astrophys.*, 550, A99.
- Zapatero Osorio M. R., Caballero J. A., Béjar V. J. S. et al. (2003) *Astron. Astrophys.*, 408, 663.
- Zapatero Osorio M. R., Martín E. L., Bouy H. et al. (2006) *Astrophys. J.*, 647, 1405.